Modelling Controller Design and Simulation of Vehicle Suspension System with Active and Semi-active dampers

Major Project Report

Submitted in partial fulfillment of the requirements for the award of the degree

Bachelor of Technology

in

Electrical and Electronics Engineering

By

Sukriti Singh, 14EE150

Sukanya Sundaram, 14EE247

Under the guidance of

Dr. Sheron Figarado

Professor

Department of Electrical and Electronics Engineering

National Institute of Technology Karnataka

DECLARATION

We hereby declare that the Project work entitled: Modelling Controller Design and Simulation of Vehicle Suspension taken up as a Major Project to the Department of Electrical and Electronics Engineering is a record of original work done by our team under the guidance of: Dr Sheron Figarado, Assistant Professor Department of Electrical and Electronics Engineering, NITK Surathkal.

All the material and information included in the report and analysis have been duly acknowledged.

The results embodied in this study have not been submitted to any other University or Institute for the award of any degree.

Date – 22nd April, 2018

Name of Team Members:

Sukriti Singh, 14EE150

Sukanya Sundaram, 14EE247

ACKNOWLEDGEMENT

It is our privilege to express our heartfelt gratitude to our guide Dr. Sheron Figarado, Assistant Professor, Department of Electrical and Electronics Engineering, National Institute of Technology Karnataka, Surathkal for giving us an opportunity to work on the project - "Modelling Controller Design and Simulation of Vehicle Suspension System with Active and Semi-active dampers".

We thank our families and our friends for their motivation, encouragement and moral support throughout the duration of the major project.

Sukriti Singh, 14EE150

Sukanya Sundaram, 14EE247

INDEX

LIST OF FIGURES

BACKGROUND

The previous semester we worked on understanding the sliding mode control as an effective control strategy and further applied to a quarter car active model to compare the results of SMC to a passive model. Our results showed a significant improvement in control when SMC was applied over passive and thus its effectiveness was proven.

This semester we extended our work applying the SMC to half car active model and a similar analysis of SMC Vs Passive was performed. To check its effectiveness on a semi active suspension model, we modelled a quarter car semi-active model on SIMULINK which employed sliding mode control as the control strategy. Once again, the SMC and Passive results were compared and analyzed and based on this, conclusions were drawn.

CHAPTER 2

2.1 INTRODUCTION

A new method is analyzed for modeling an active suspension system for half-car model in state space form and to develop a robust strategy in controlling the active suspension system. Proportional integral sliding mode control strategy is proposed for the system.

2.2. WHY ACTIVE OVER PASSIVE SUSPENSION SYSTEMS?

The passive suspension system, which approach optimal characteristics, had offered an attractive choice for a vehicle suspension system and had been widely used for passengers. However, the suspension spring and damper do not provide energy to the suspension system and control only the motion of the car body and wheel by limiting the suspension velocity according to the rate determined by the designer. To overcome the above problem, active suspension systems have been proposed by various researchers. Active suspension systems dynamically respond to changes in the road profile because of their ability to supply energy that can be used to produce relative motion between the body and wheel.

Typically, active suspension systems include sensors to measure suspension variables such as body velocity, suspension displacement, wheel velocity and wheel or body acceleration. An active suspension is one in which the passive components are augmented by actuators that supply additional forces. These additional forces are determined by a feedback control law using data from sensors attached to the vehicle.

2.3 MODELLING OF HALF CAR

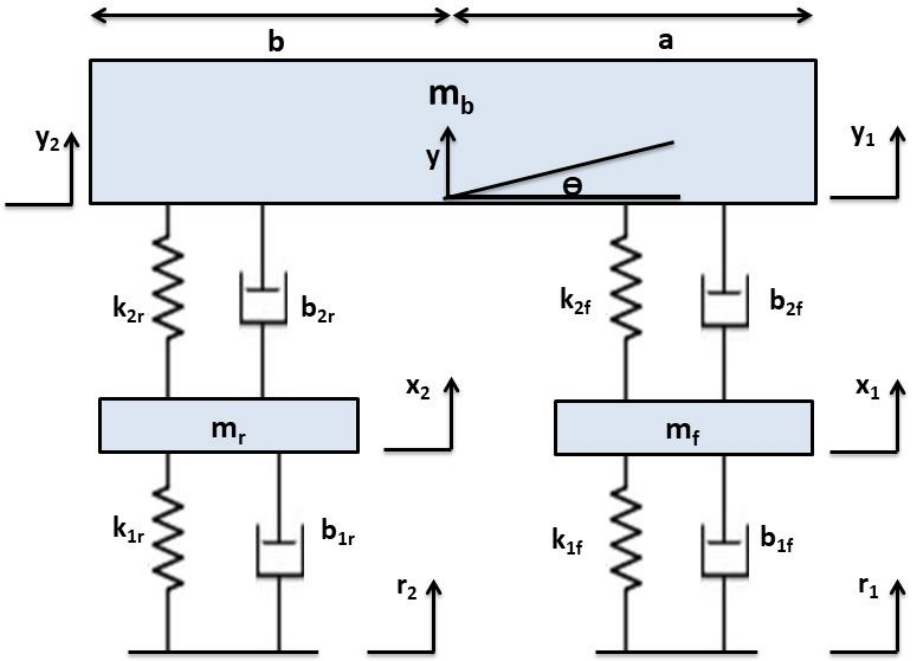

Fig 2.1: Half Car model

m_b = mass of car body (sprung mass)
m_f = mass of front wheel (unsprung mass)
mr = mass of rear wheel (unsprung mass)
k_{1f} : spring constant of front wheel and tyre
k_{1r} : spring constant of rear wheel and tyre
k_{2f}: spring constant of front suspension system
k_{2r} : spring constant of rear suspension system
b_{1f} : damping constant of front wheel and tyre
b_{1r} : damping constant of rear wheel and tyre
b_{2f} : damping constants of front suspension system
b_{2r} : damping constants of rear suspension system
J: Moment of Inertia of half car
a, b : lengths to front and rear respectively
Θ : pitch
$y_1 = y + a \tan \Theta = y + a \Theta$ (approx.., since Θ is very small)
$y_2 = y - b \tan \Theta = y - b \Theta$ (approx.., since Θ is very small)

Free Body Diagram of front wheel

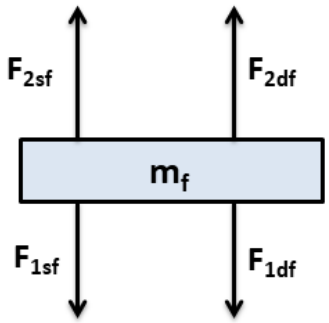

Fig 2.2: FBD of front wheel

F_{1sf} , F_{2sf} = Forces due to springs

F_{1df} , F_{2df} = Forces due to dampers

Equations from the free-body diagram:

$m_f \ddot{x_1} = F_{2sf} + F_{2df} - F_{1sf} - F_{1df}$

$m_f \ddot{x_1} = k_{2f} (y_1 - x_1) + b_{2f} (\dot{y_1} - \dot{x_1}) - k_{1f} (x_1 - r_1) - b_{1f} (\dot{x_1} - \dot{r_1})$

Substituting for $y_1 = y + a \Theta$,

$m_f \ddot{x_1} = k_{2f} y + k_{2f} a \Theta - k_{2f} x_1 + b_{2f} \dot{y} + b_{2f} a \dot{\theta} - b_{2f} \dot{x_1} - k_{1f} x_1 + k_{1f} r_1 - b_{1f} \dot{x_1} + b_{1f} \dot{r_1}$

Rearranging gives:

$- k_{2f}\, y - b_{2f}\, \dot{y} - k_{2f}\, a\, \Theta - b_{2f}\, a\, \dot{\theta} + m_f \ddot{x_1} + k_{2f}\, x_1 + k_{1f}\, x_1 + b_{2f}\, \dot{x_1} + b_{1f}\, \dot{x_1} = k_{1f}\, r_1 + b_{1f} \dot{r_1}$ (i)

Similarly for rear wheel and substituting y2 = y - b Θ and rearranging,

$- k_{2r}\, y - b_{2r}\, y' + k_{2r}\, b\, \Theta + b_{2r}\, b\, \Theta' + m_r\, \ddot{x_2} + k_{2r}\, x_2 + k_{1r}\, x_2 + b_{2r}\, \dot{x_2} + b_{1r}\, \dot{x_2} = k_{1r}\, r_2 + b_{1r}\, r2'$ (ii)

Free Body Diagram of suspension system

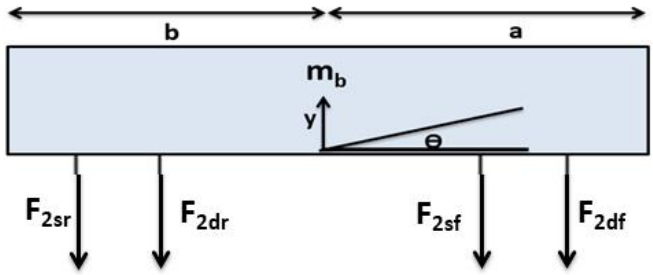

Fig 2.3: FBD of suspension system

Equations from the free-body diagram:

$m_b\, \ddot{y} = - k_{2f}(y_1 - x_1) - b_{2f}(\dot{y_1} - \dot{x_1}) - k_{2r}\,(y_2 - x_2) - b_{2r}\,(y2' - x2')$

Substituting for (y1 = y + a Θ) and (y2 = y - b Θ),

$m_b\, \ddot{y} = - k_{2f}\, y - k_{2f}\, a\, \Theta + k_{2f}\, x_1 - b_{2f}\, \dot{y} - b_{2f}\, a\, \dot{\theta} + b_{2f}\, \dot{x_1} - k_{2r}\, y + k_{2r}\, b\, \Theta + k_{2r}\, x_2 - b_{2r}\, \dot{y}$

$+ b_{2r}\, b\, \dot{\theta} + b_{2r}\, \dot{x_2}$

Rearranging,

$k_{2f}\, y + k_{2r}\, y + b_{2f}\, \dot{y} + b_{2r}\, y' + m_b\, \ddot{y} + k_{2f}\, a\, \Theta - k_{2r}\, b\, \Theta + b_{2f}\, a\, \dot{\theta} - b_{2r}\, b\dot{\theta} - k_{2f}\, x_1 - b_{2f}\dot{x_1} - k_{2r}\, x_2 - b_{2r}\, \dot{x_2} = 0$ (iii)

From the above,

$J\, \ddot{\theta} = a\,(- k_{2f}\,(y_1 - x_1) - b_{2f}\,(\dot{y_1} - \dot{x_1})) - b\,(- k_{2r}\,(y_2 - x_2) - b_{2r}\,(\dot{y_2} - \dot{x_2}))$

Substituting for ($y_1 = y + a\, \Theta$) and ($y_2 = y - b\, \Theta$) and rearranging,

$k_{2f}\, a\, y - k_{2r}\, b\, y + b_{2f}\, a\, \dot{y} - b_{2r}\, b\, \dot{y} + J\, \ddot{\theta} + k_{2f}\, a_2\, \Theta + k_{2r}\, b_2\, \Theta + b_{2f}\, a_2\, \dot{\theta} + b_{2r}\, b_2\, \dot{\theta} - k_{2f}\, a\, x_1 - b_{2f}\, a\, \dot{x_1} + k_{2r}\, b\, x_2 + b_{2r}\, b\, \dot{x_2} = 0$ (iv)

Assumptions:

Consider the model of a passenger's car subject to irregular excitation from a road surface. This model has been used in the design of active suspension system. The motion equations of the half-car model is represented in a vector matrix form as follows: The motion equations of the half car are represented in a vector matrix form as follows:

$$M\ddot{x} + Sx + Tx = Du + Er \quad (1)$$

Where the state, active control and excitation vectors are given by:

$$x = [y_1 \;\; x_1 \;\; y_2 \;\; x_2 \;\; \dot{y_1} \;\; \dot{x_1} \;\; \dot{y_2} \;\; \dot{x_2}]^T$$

$$u = [u_f \;\; u_r]^T$$

$$r = [\, r_1 \;\; r_2]^T$$

And

$$M = \begin{pmatrix} (bm_b)/L & 0 & (am_b)/L & 0 \\ I_b/L & 0 & -I_b/L & 0 \\ 0 & m_1 & 0 & 0 \\ 0 & 0 & 0 & m_2 \end{pmatrix}$$

$$S = \begin{pmatrix} b_{2f} & -b_{2f} & b_{2r} & b_{2r} \\ a(b_{2f}) & -a(b_{2f}) & -b(b_{2r}) & b(b_{2r}) \\ -b_{2f} & b_{2f} & 0 & 0 \\ 0 & 0 & -b_{2r} & b_{2r} \end{pmatrix}$$

$$T = \begin{pmatrix} k_{2f} & -k_{2f} & k_{2r} & -k_{2r} \\ a(k_{2f}) & -a(k_{2f}) & -b(k_{2r}) & -b(k_{2r}) \\ -k_{2f} & (k_{2f} + k_{1f}) & 0 & 0 \\ 0 & 0 & (-k_{2r}) & (k_{2r} + k_{1r}) \end{pmatrix}$$

$$D = \begin{pmatrix} 1 & 1 \\ a & -b \\ -1 & 0 \\ 0 & -1 \end{pmatrix} \qquad E = \begin{pmatrix} 0 & 0 & 0 & 0 \\ 0 & 0 & 0 & 0 \\ k_{1f} & 0 & 0 & 0 \\ 0 & 0 & k_{1r} & 0 \end{pmatrix}$$

Where I_b is the moment of inertia for the vehicle body

Equation (1) is re-written in state space form as:

$$\dot{x(t)} = Ax(t) + Bu(t) + r(t) \quad (2)$$

Where $x(t) \in R^n$ is state vector and $u(t) \in R^m$ is the control input and $r(t)$ represents uncertainties with mismatched conditions.

2.4 SWITCHING SURFACE AND CONTROLLER DESIGN

The sliding surface is given as:

$$\sigma(t) = Cx(t) \tag{3}$$

To enter sliding mode, $\sigma(t) = 0 \rightarrow \dot{\sigma(t)} = 0$ (4)

$$\boxed{\dot{\sigma(t)} = 0} \tag{5}$$

Solving for this from equation(2),

$$\boxed{u_{eq} = (CB_{in})^{-1}(-CAx - Cr(t))} \tag{6}$$

2.5. SIMULINK MODEL OF HALF CAR WITH SMC CONTROLLED ACTIVE SUSPENSION

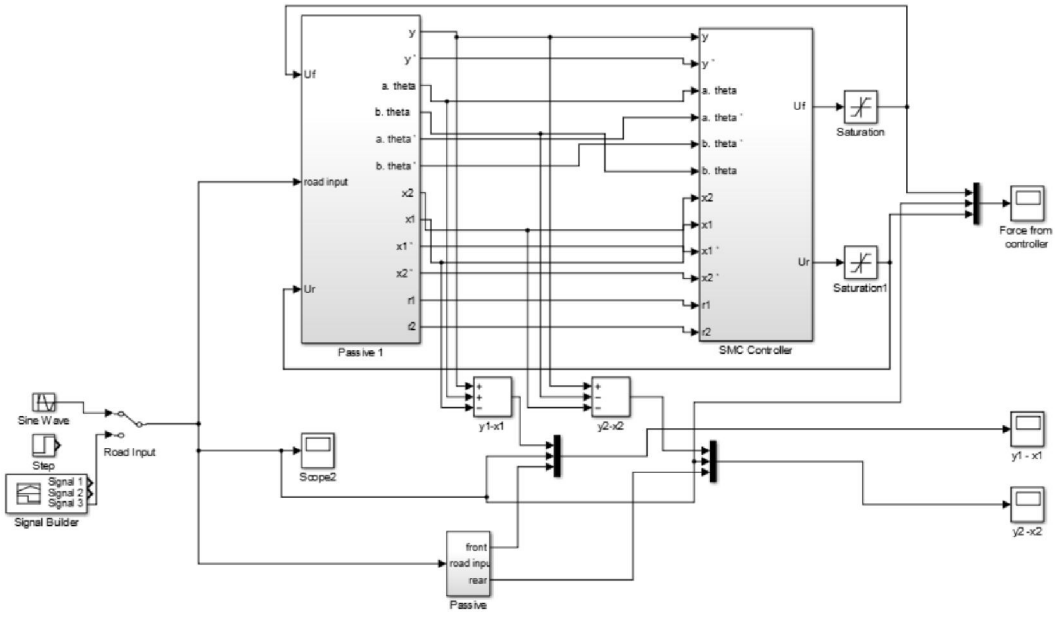

Fig: 2.4(a) Full block diagram of Half car model with SMC controlled active susepnsion

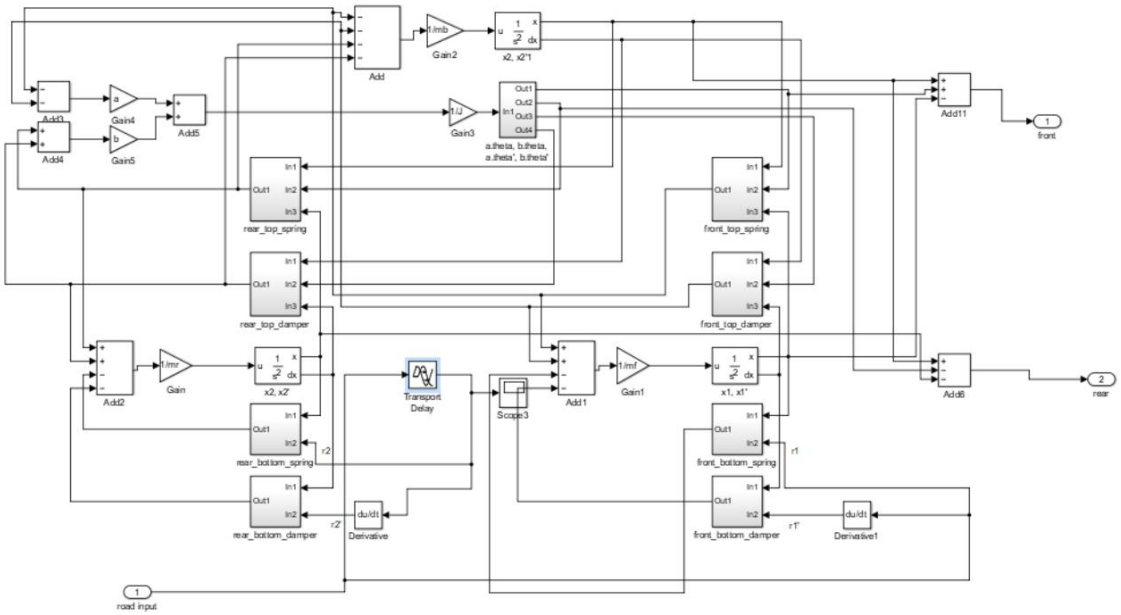

Fig 2.4(b): Passive suspension system of half car

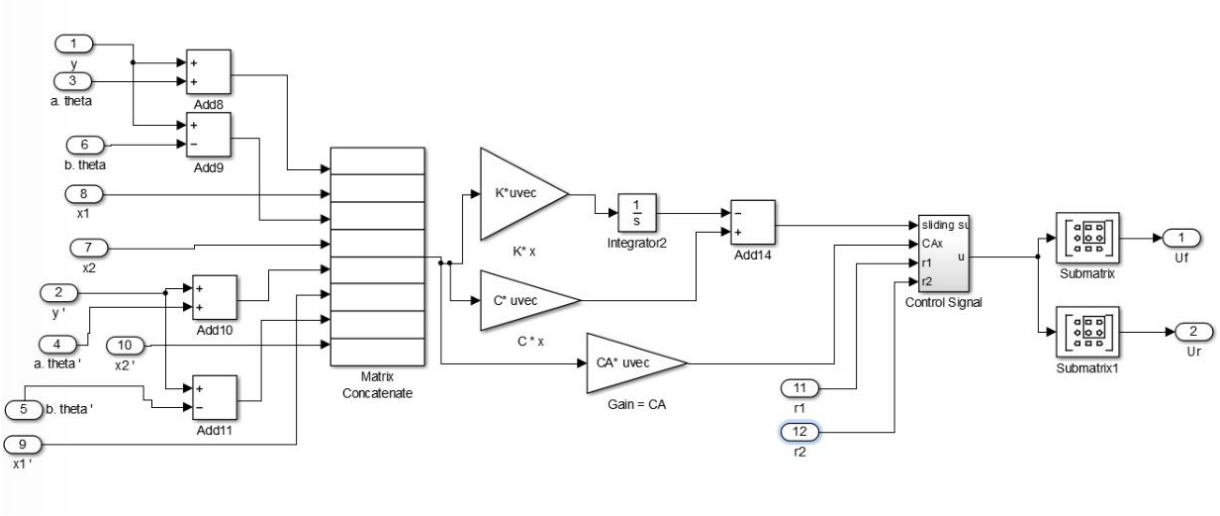

Fig: 2.4(c) SMC controller of active suspension

2.6. SIMULATION RESULTS AND ANALYSIS

The Simulink Model shown in section 2.5. was used to test the various parameters of the half car with SMC controlled active suspension for different road inputs namely sine wave, step and pulse input. The same were recorded for a half car with passive suspension in order to compare. These parameters are displacement and acceleration of sprung mass, difference in displacements of sprung and unsprung masses, and that of unsprung mass and road input was also recorded in each case.

2.6.1. Sine Wave Road Input

Displacement of sprung mass(y)

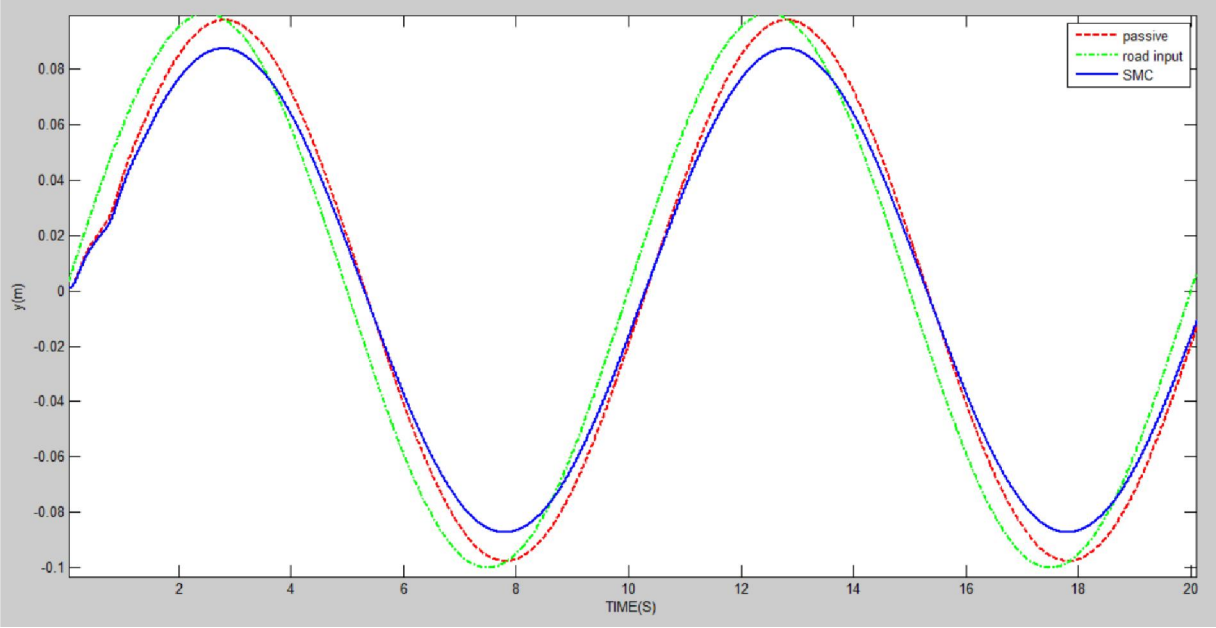

Figure 2.5: Road input-sine wave(amplitude = 0.1 m and a frequency =0.1Hz)

Figure 2.5 illustrates the response of SMC compared with Passive system when excited with a road input of Sine Wave of amplitude = 0.1 m and a frequency =0.1Hz. The overshoot of the passive system is 0.098m vs SMC which is 0.086m. Hence SMC has proven to be a better control strategy.

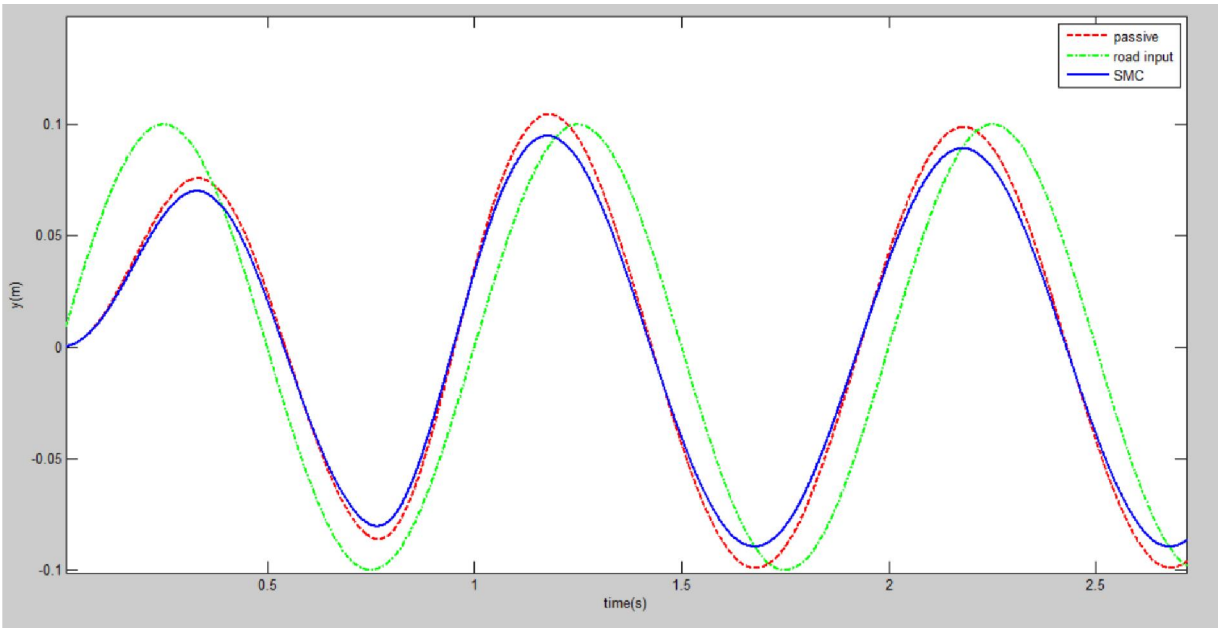

Figure 2.6: Road input-sine wave(amplitude = 0.1 m and a frequency =1Hz)

Figure 2.6 illustrates the response of SMC compared with Passive system when excited with a road input of Sine Wave of amplitude = 0.1 m and a frequency =1Hz. The overshoot of the passive system is 0.078m vs SMC which is 0.069m.

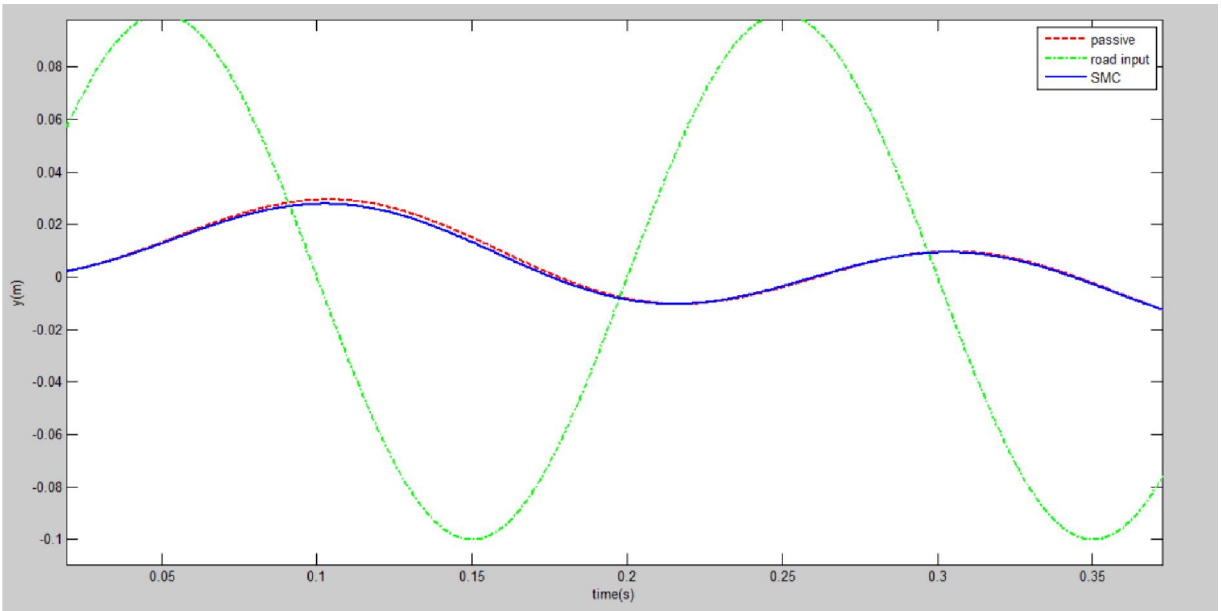

Figure 2.7: Road input-sine wave(amplitude = 0.1 m and a frequency =5 Hz)

Figure 2.7 illustrates the response of SMC compared with Passive system when excited with a road input of Sine Wave of amplitude = 0.1 m and a frequency =1Hz. The overshoot of both is very similar differing by just 0.02m.

A similar pattern is observed at higher frequencies.

Difference in the displacements of sprung and unsprung mass: $(y_1 - x_1)$-Front

The road input was taken as sine wave with amplitude of 0.1m and frequency was varied from 0.1 Hz to 20 Hz for the front wheel.

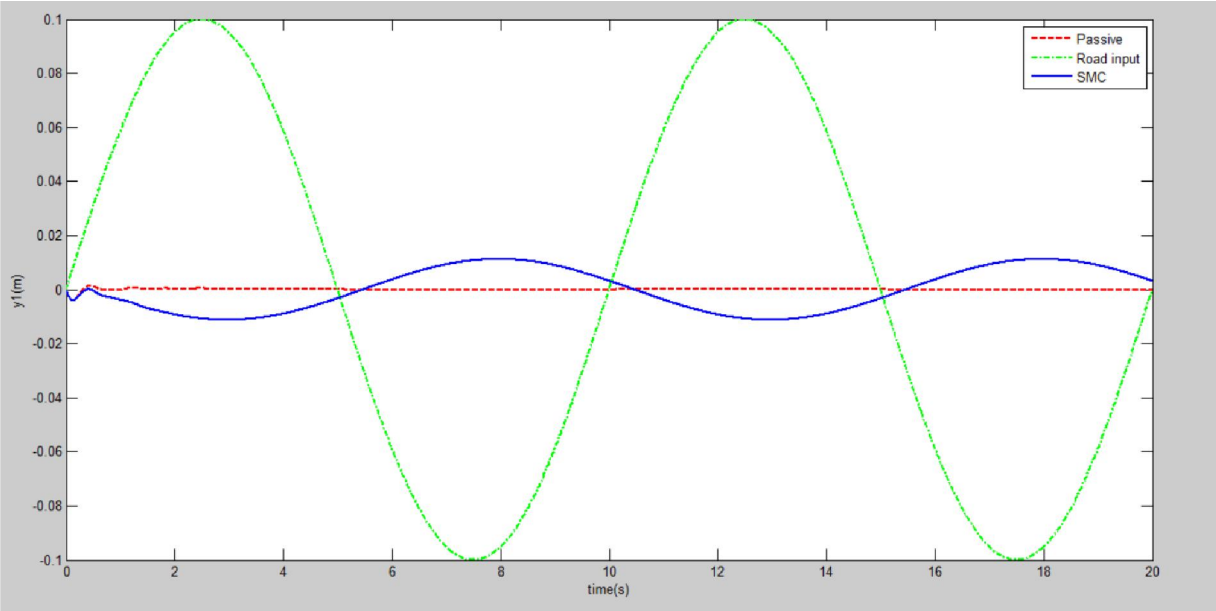

Fig 2.8:Input: Sine wave (0.1 m, 0.1Hz)

Figure 2.8 illustrates the response of SMC compared with Passive system when excited with a road input of Sine Wave of amplitude = 0.1 m and a frequency =0.1Hz. Although the overshoot of SMC system is slightly higher than the passive system on both the positive and negative fronts, i.e., 0.011m and -0.012m, the former settles as a sine wave.

Sine waves with varied frequencies were analyzed for the displacement of sprung mass. These have been illustrated in the Figures 2.8-2.10.

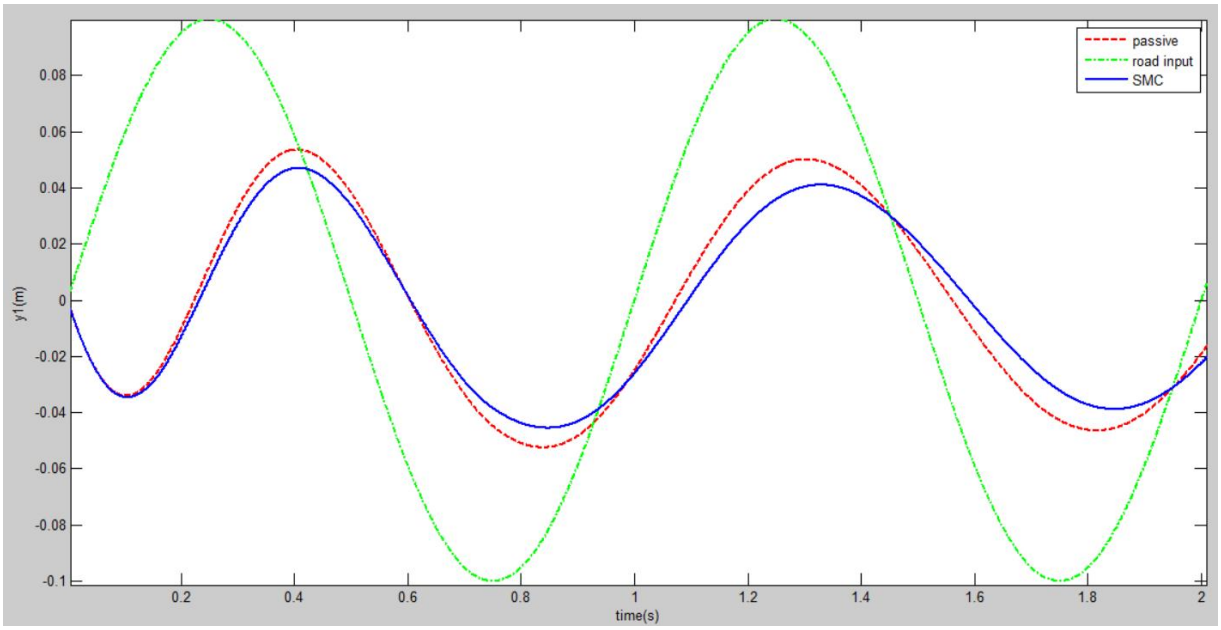

Fig 2.9: Input: Sine wave (0.1 m, 1Hz)

The maximum overshoot of y for the SMC system here is lower than passive, i.e. (0.048m-SMC and 0.04m-Passive) .

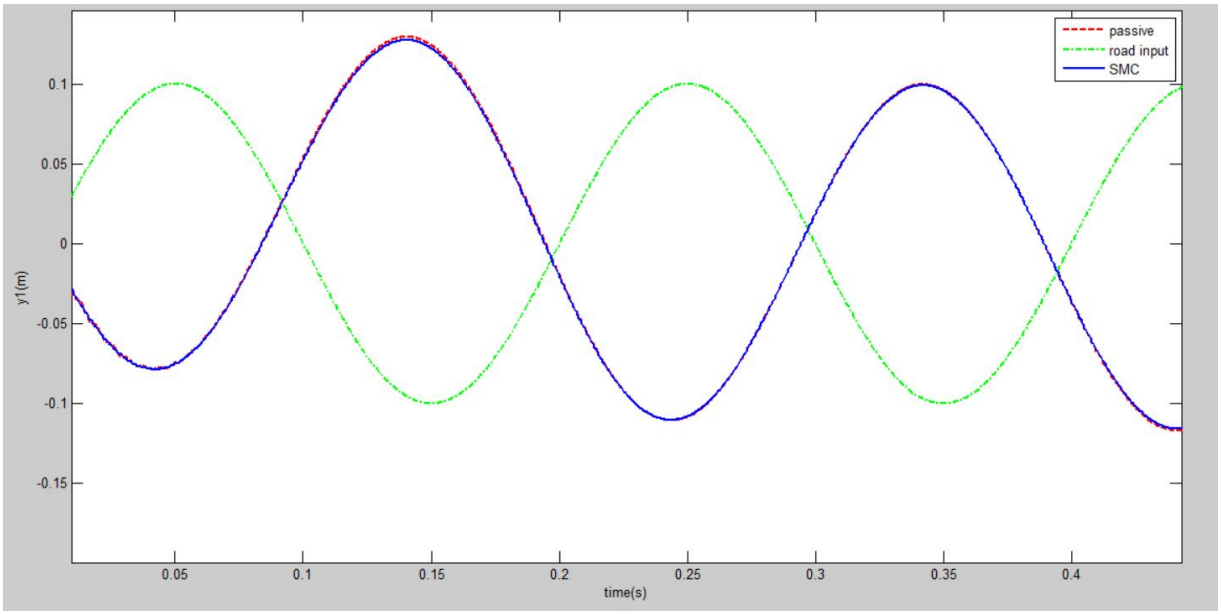

Fig 2.10: Input: Sine wave (0.1 m, 5Hz)

In Fig 2.7, the passive and the SMC produce almost similar outputs with outputs of 0.125m(passive) and 0.12m(SMC)

A similar pattern can be observed for sine waves of higher frequencies.

Difference in the displacements of sprung and unsprung mass: $(y_2 - x_2)$-Rear

The road input was taken as sine wave with amplitude of 0.1m and frequency was varied from 0.1 Hz to 20 Hz for the difference in the displacements of sprung and unsprung masses for rear wheel and a similar analysis was performed.

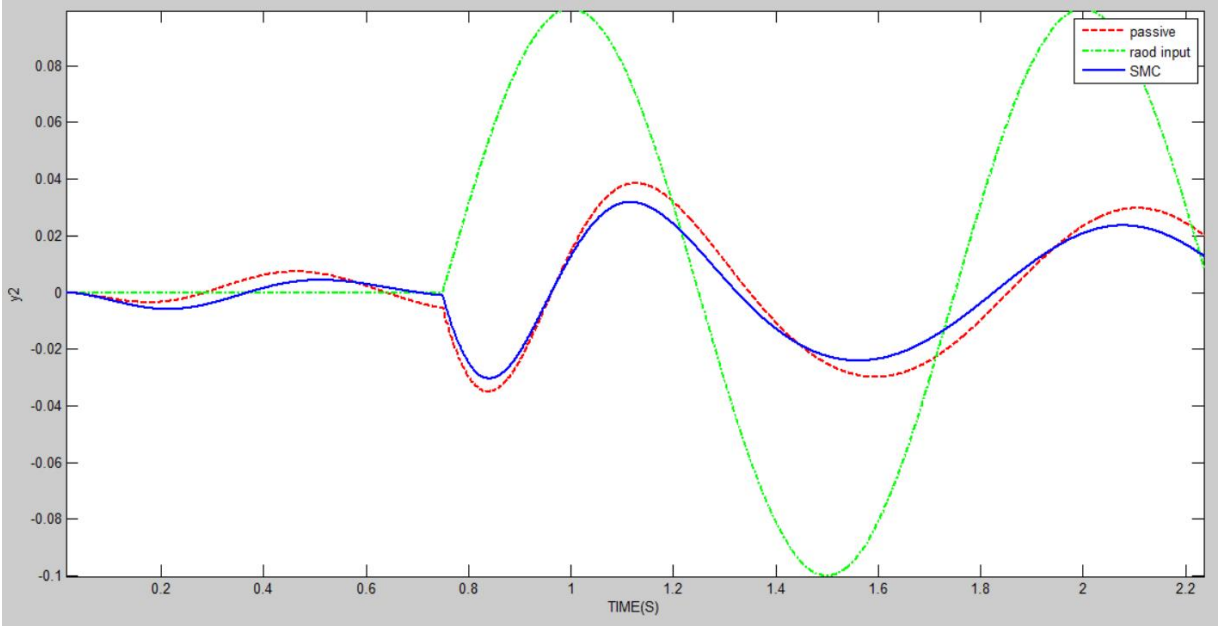

Fig 2.11: Input: Sine wave (0.1 m, 1Hz)

The rear wheel is fed input with a delay of 0.75 seconds. The passive system peaks at 0.04m while the SMC at 0.03m.

Difference in displacements of unsprung mass and road input (x_1-r_1)-Front

The aim of the SMC controller was to increase road comfort by reducing the deflection of the sprung mass. However, the same has an effect on the road handling too which is reflected by the difference in displacements of unsprung mass and the road input. The same is studied for sine waves of three different frequencies in the figures 2.12-2.13.

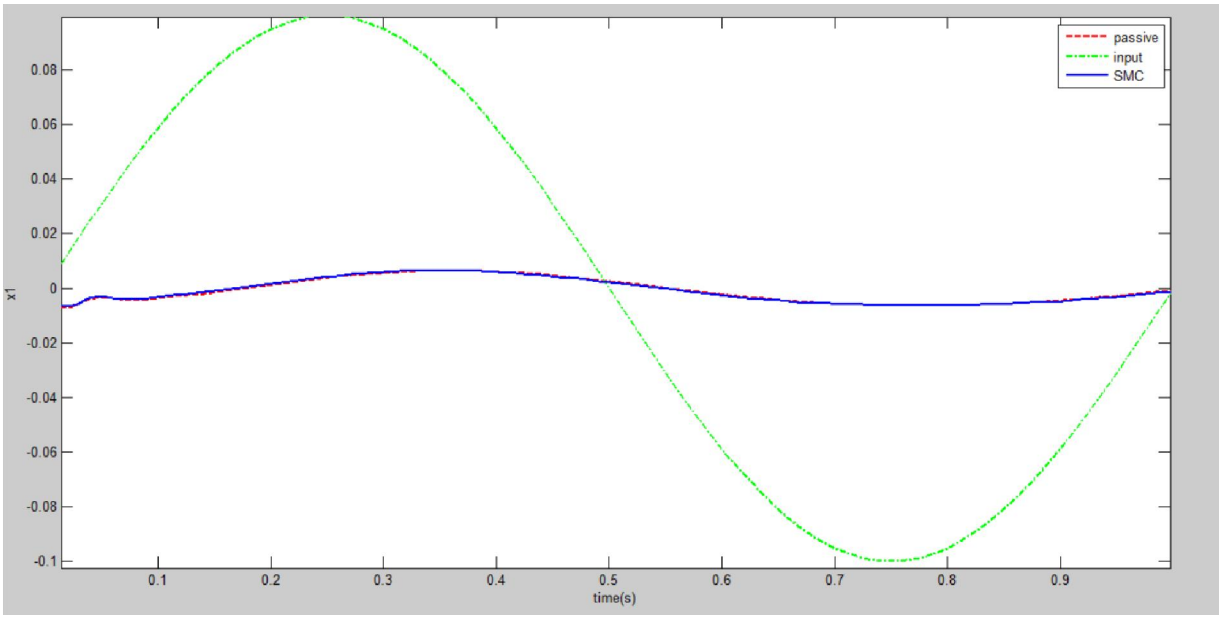

Fig 2.12:Road input-Sine wave(0.1 m, 1Hz)

Fig 2.12 shows that the output for SMC and the passive system is very similar with a peaking value of 0.007m.

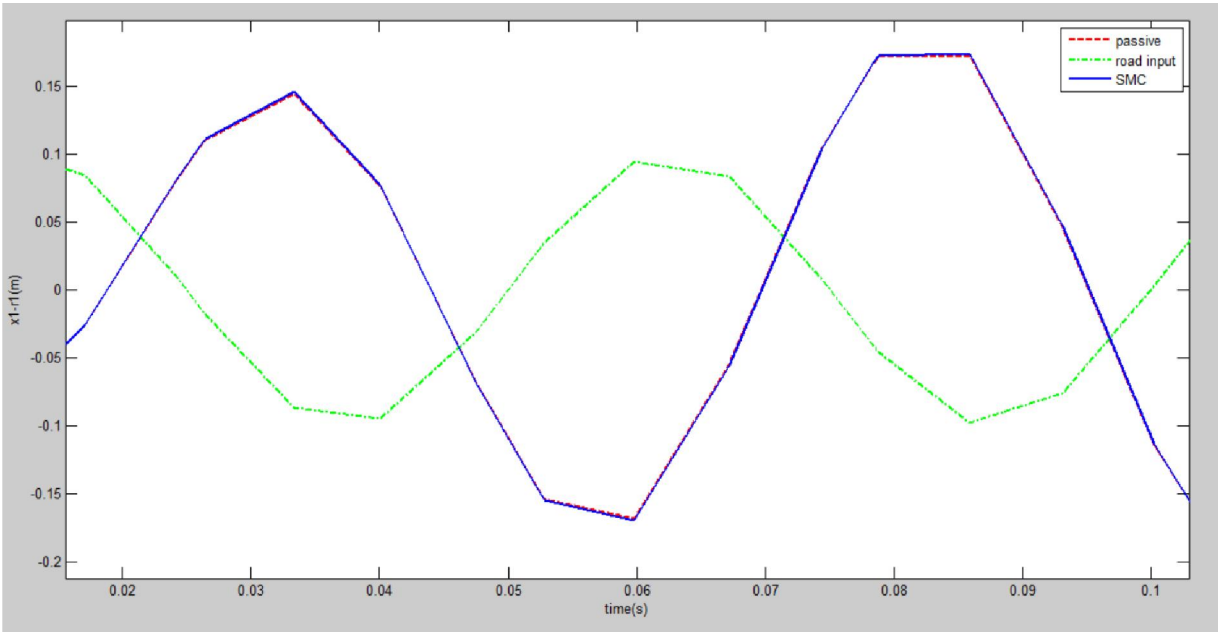

Fig 2.13:Road input-Sine wave(0.1 m, 20Hz)

Fig 2.13 Shows that with increasing frequency the shape of the sine wave slightly distorts. However, the values of SMC and passive output still remain very similar(0.0145m)

Performing the same analysis for x_2-r_2, we get the following graph.

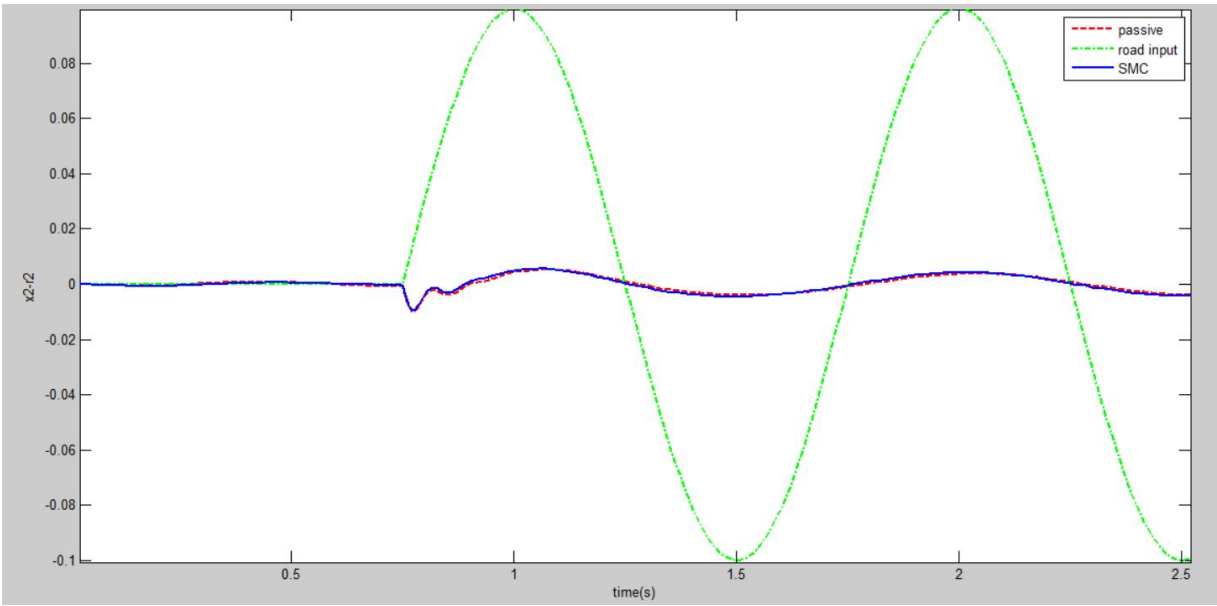

Fig 2.14 -Road input-sine wave(0.1 m and 1Hz)

The rear wheel is fed input with a delay of 0.75 seconds. The outputs then obtained are similar to the previous case of front wheel and road input displacement.

Vertical acceleration of Sprung mass (ÿ)

Besides the displacement of sprung mass, the vertical acceleration of the same also plays an important role in determining the extent of road comfort of a vehicle.

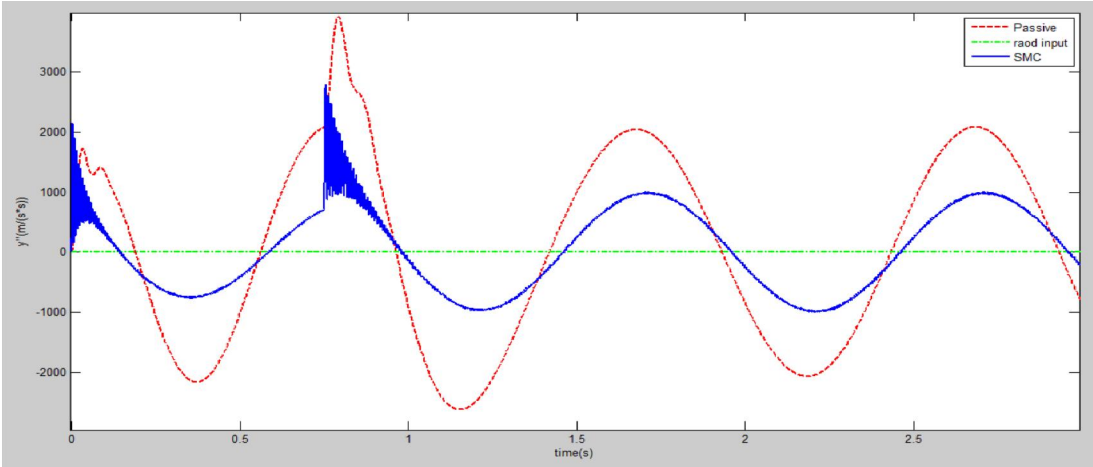

Fig 2.15: Input: Sine wave (0.1 m, 1Hz)

Figure 2.15 illustrates the vertical acceleration of sprung mass (m/s^2) of SMC compared with Passive system when excited with a road input of Sine Wave of amplitude = 0.1 m and a frequency = 1Hz. The maximum overshoot of SMC system is 2800 m/s^2 which in 3 seconds comes down to non-sinusoidal oscillations of maximum amplitude 1000 m/s^2.

Sine waves with varied frequencies were analyzed for the acceleration of sprung mass. These have been illustrated in the Figures 2.16-2.17.

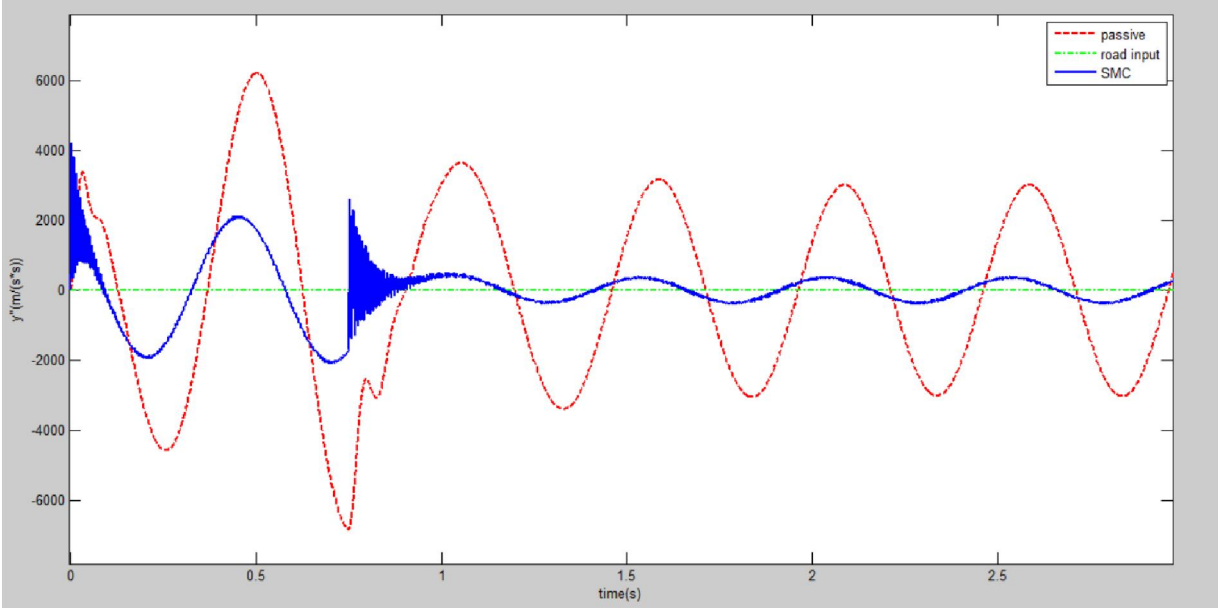

Fig 2.16: Input: Sine wave (0.1 m, 2Hz)

In Figure 2.16, the maximum overshoot of SMC system is 4200 m/s^2 when compared to 6200 m/s^2 of passive system. The SMC controller gives undesirable vertical acceleration of sprung mass at lower frequencies. Also, an overshoot is seen at a zero crossing of the road input which takes 50% of the time till next zero-crossing to settle.

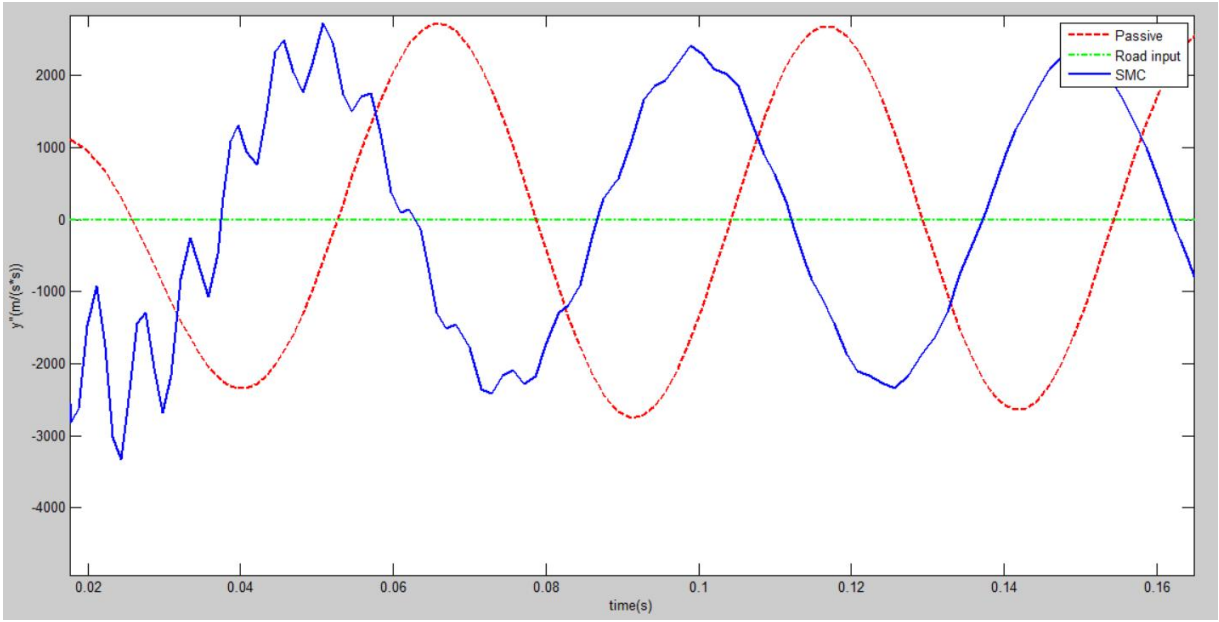

Fig 2.17: Input: Sine wave (0.1 m, 20Hz)

In Fig. 2.17, the maximum overshoot of SMC system is 2750 m/s^2 which in 0.054 seconds comes down to non-sinusoidal oscillations of maximum amplitude 2450 m/s^2.

Force exerted by controller (N)

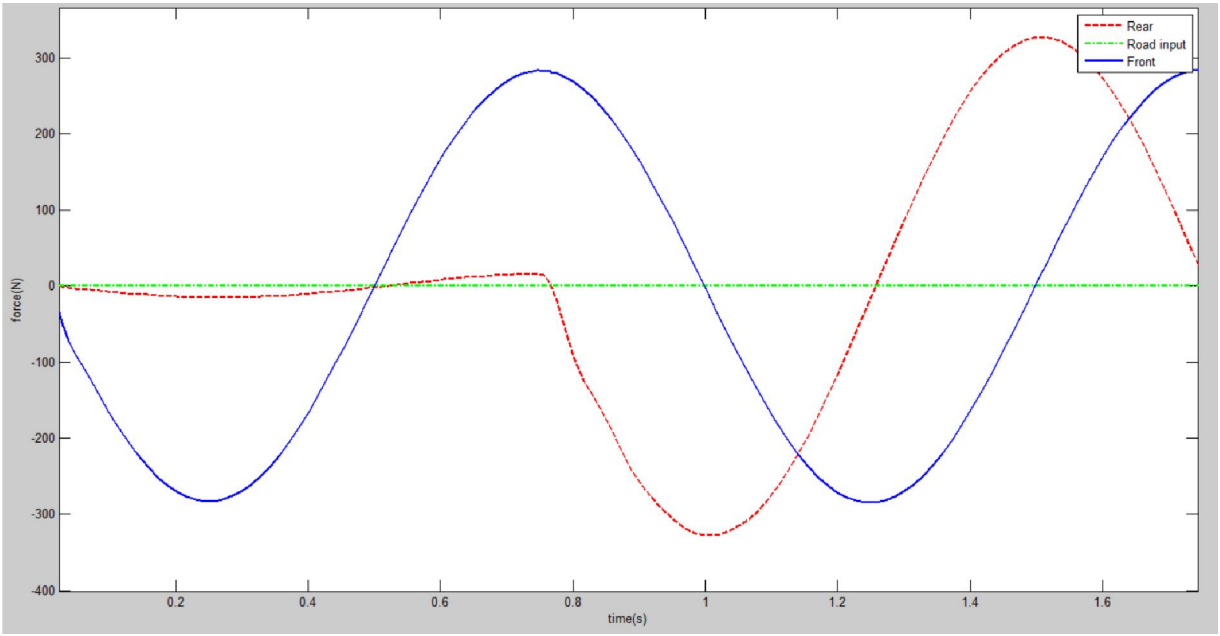

Fig 2.18 : Input-Sine wave (Amplitude-0.1, frequency-1 Hz)

In fig 2.18, the force exerted by the front wheel peaks at 282N while the force exerted by the rear wheel peaks at 312N.

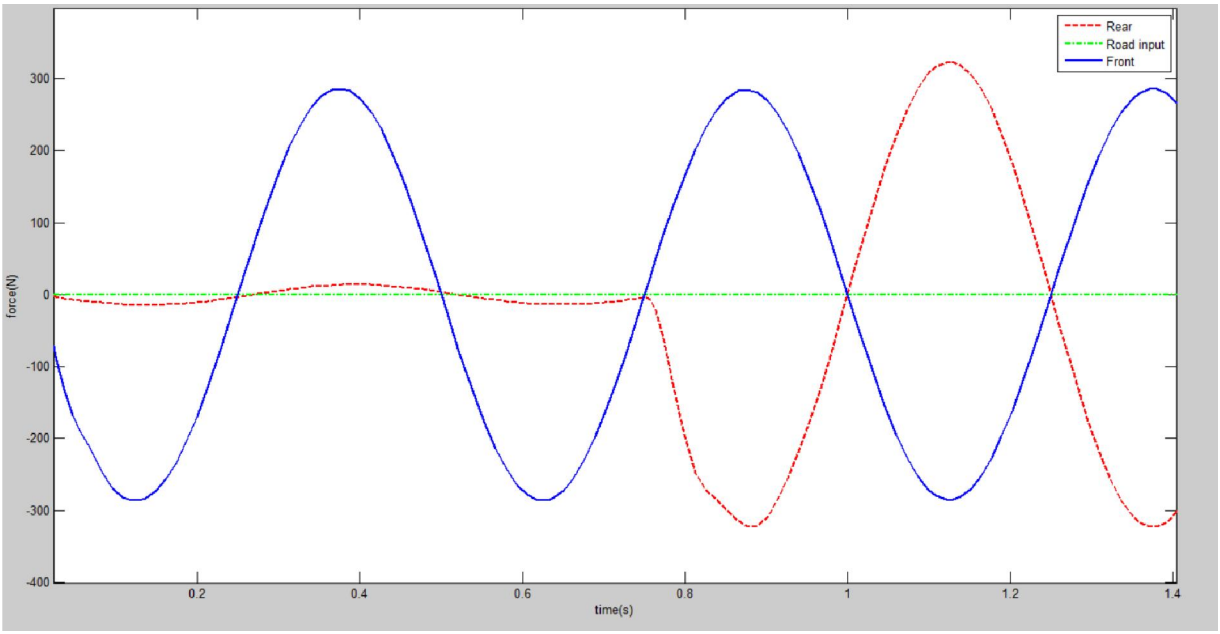

Fig 2.19:Input-Sine wave (Amplitude-0.1, frequency-2 Hz)

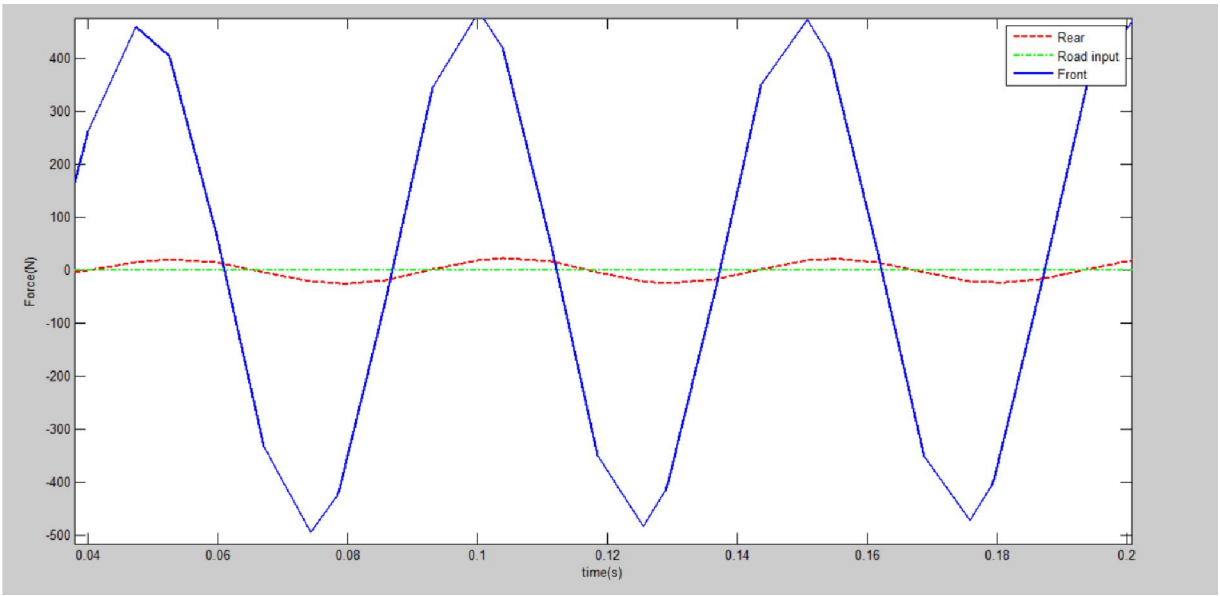

Fig 2.20 :Input-Sine wave (Amplitude-0.1, frequency-20Hz)

Pitch

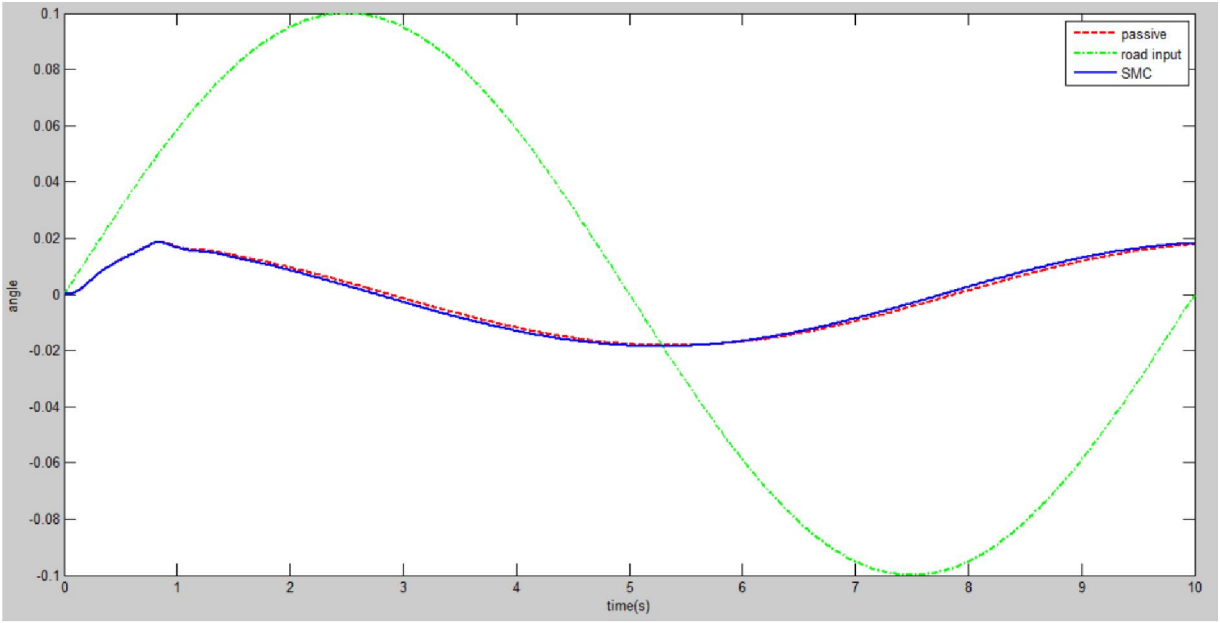

Fig 2.21 :Input-Sine wave (Amplitude-0.1, frequency-0.1Hz)

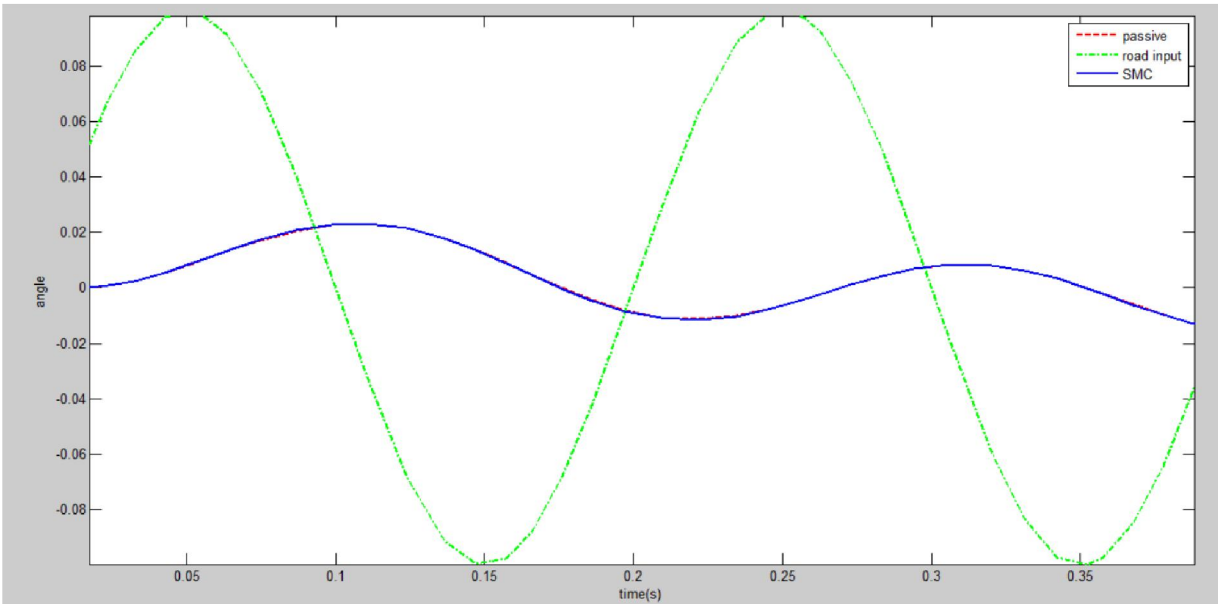

Fig 2.22 :Input-Sine wave (Amplitude-0.1, frequency-5Hz)

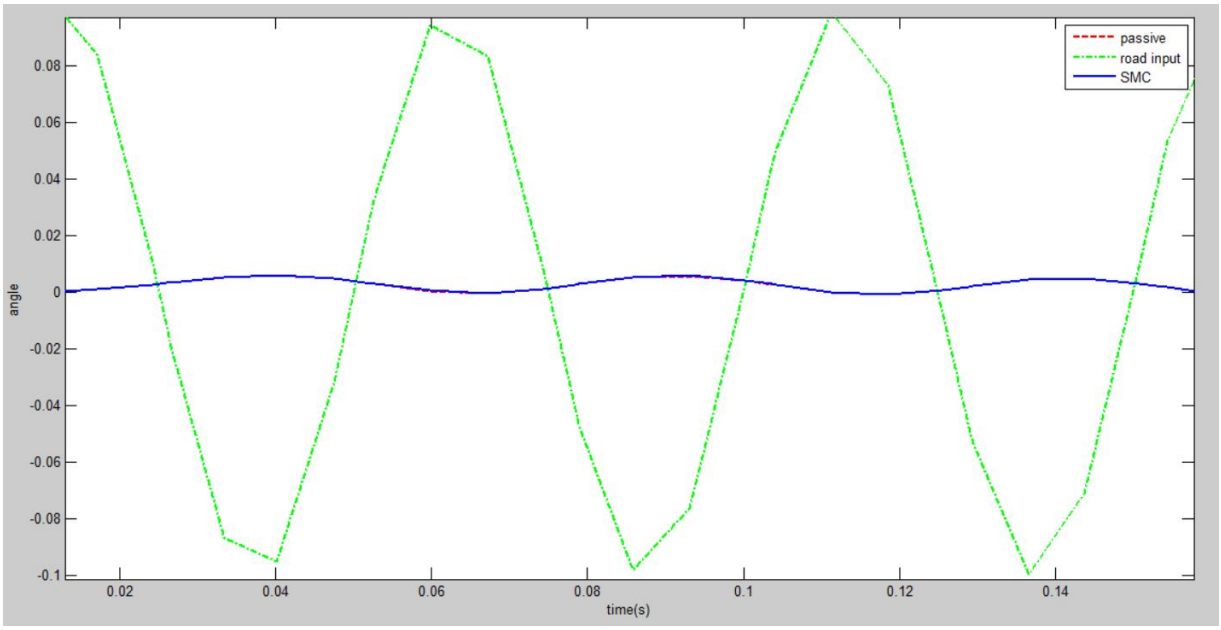

Fig 2.23 :Input-Sine wave (Amplitude-0.1, frequency-20Hz)

From Figs2.21-2.23, we can analyze that with increasing frequency, the pitch for SMC reduces, so the disturbances felt by the passengers will be lesser than in passive case.

2.6.2 Pulse Input

The road input was taken as a pulse with amplitude of 0.1m and width of 0.5s.

Displacement of sprung mass (y)

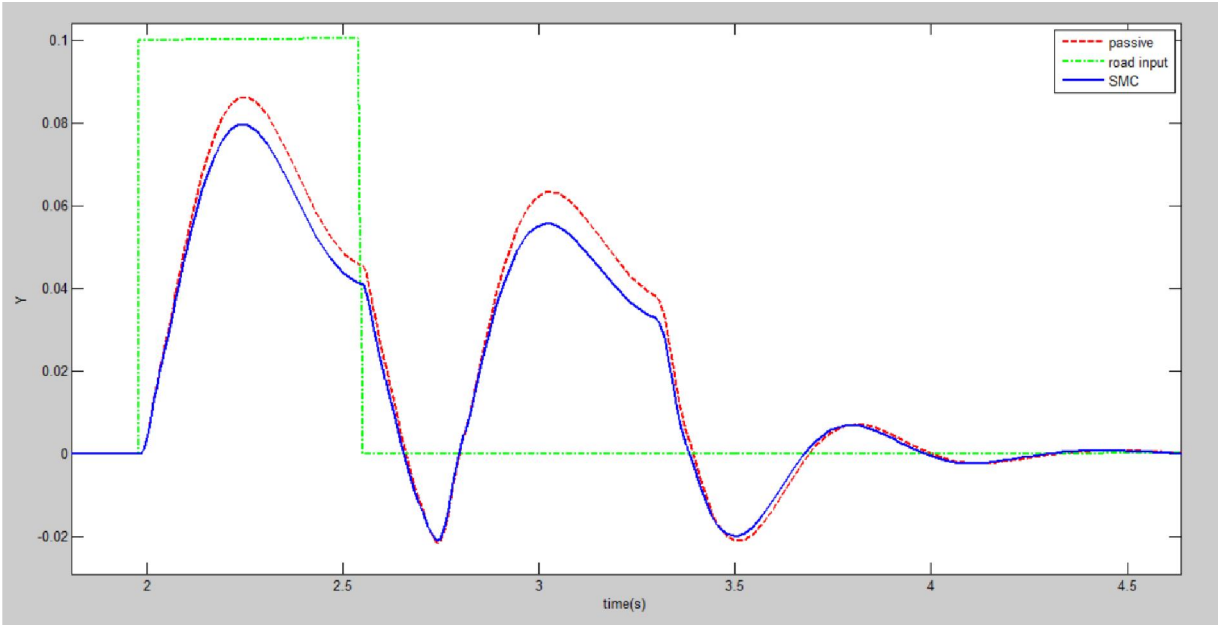

Fig 2.24: Pulse input with amplitude 0.1m and width 0.5s

In Figure 2.24, it is seen that the maximum overshoot of the output of the SMC system is less than the passive system in both the positive and negative directions, i.e., 0.075m and -0.02m for SMC and 0.085 and -0.022m for passive system. The settling time for SMC is almost twice as that of the passive system.

Difference in displacement of front sprung and unsprung mass (y_1-x_1)

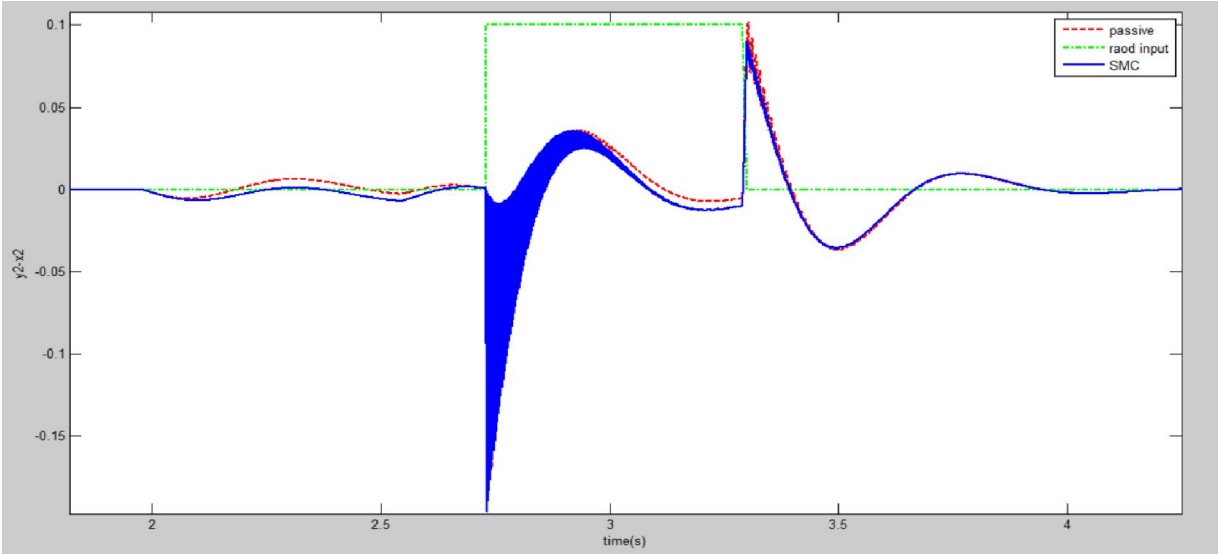

Fig 2.25: Pulse input with amplitude 0.1m and width 0.5s

Difference in displacement of rear sprung and unsprung mass (y_2-x_2)

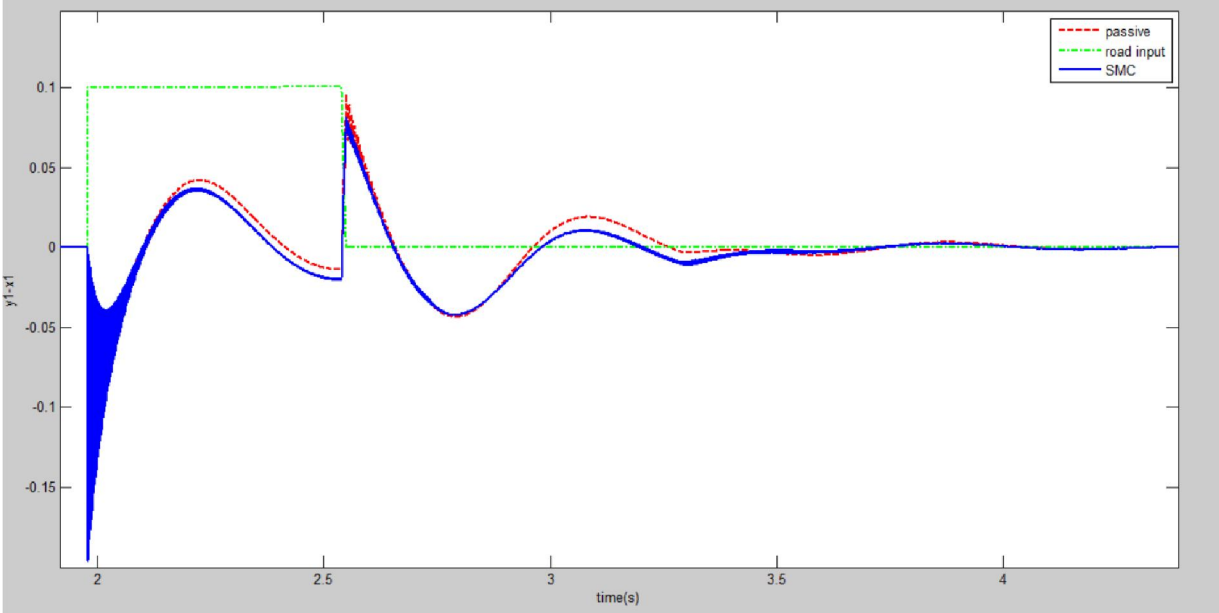

Fig2.26: Pulse input with amplitude 0.1m and width 0.5s

From figs 2.25 and 2.26, it is clear that the front and rear wheel displacements are very similar except for a time lag of 0.75s for the rear wheel.

Difference in displacement of front unsprung mass and road input (x_1-r_1)

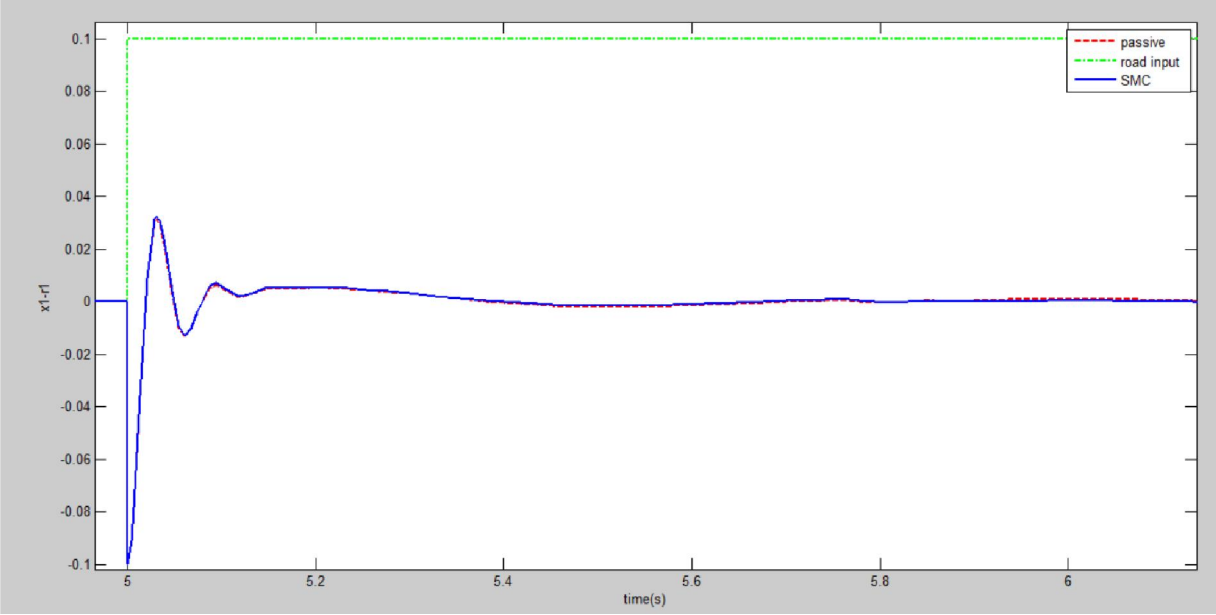

Fig2.27: Pulse input with amplitude 0.1m and width 0.5s

Difference in displacement of rear unsprung mass and road input (x_2-r_2)

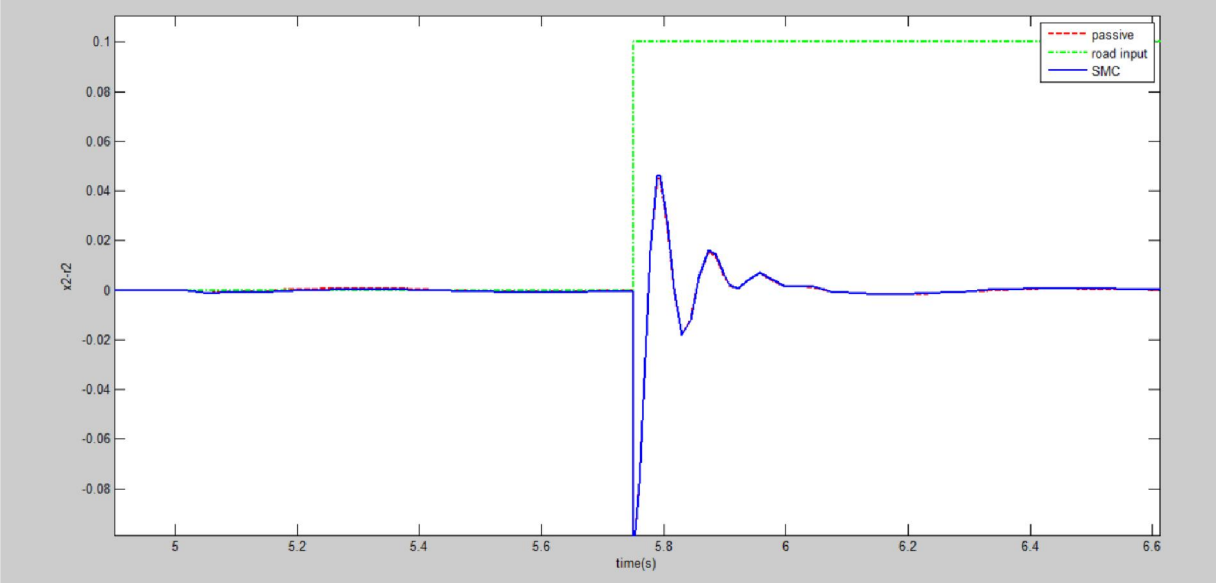

Fig2.28: Pulse input with amplitude 0.1m and width 0.5s

From figs 2.27 and 2.28, it is clear that the front and rear wheel displacements is similar except for a time lag of 0.75s for the rear wheel. Peak value of SMC for front wheel is 0.038m and for rear it is 0.053m.

Acceleration of sprung mass (ÿ)

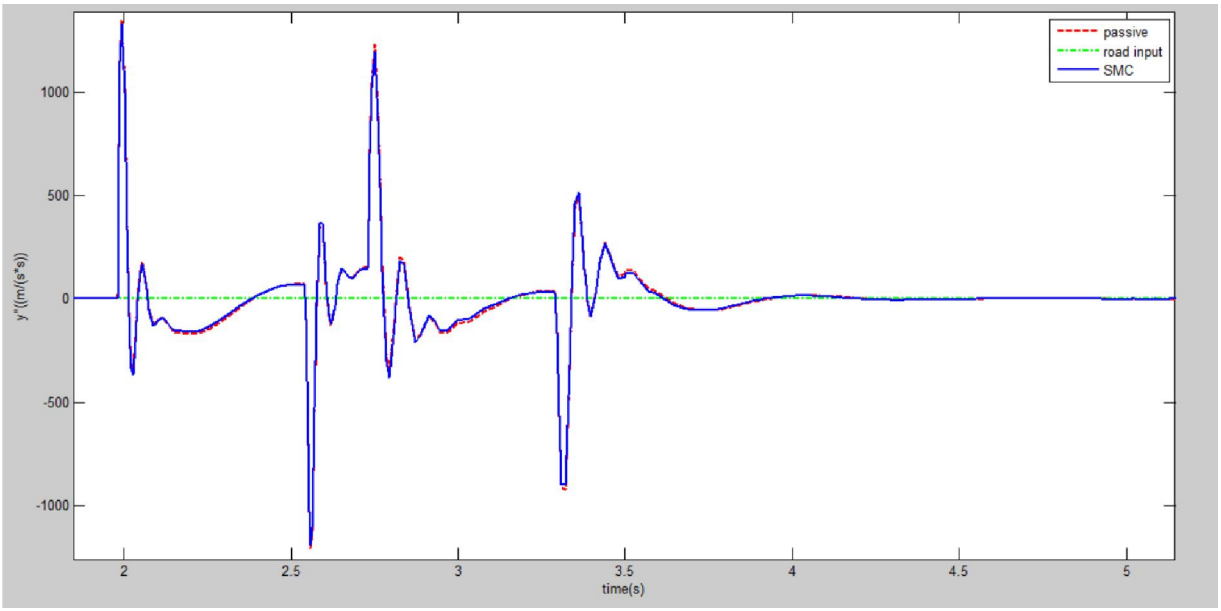

Fig2.29: Pulse input with amplitude 0.1m and width 0.5s

From fig 2.29, the acceleration initially peaks and there are distortions, after which it settles.

Pitch

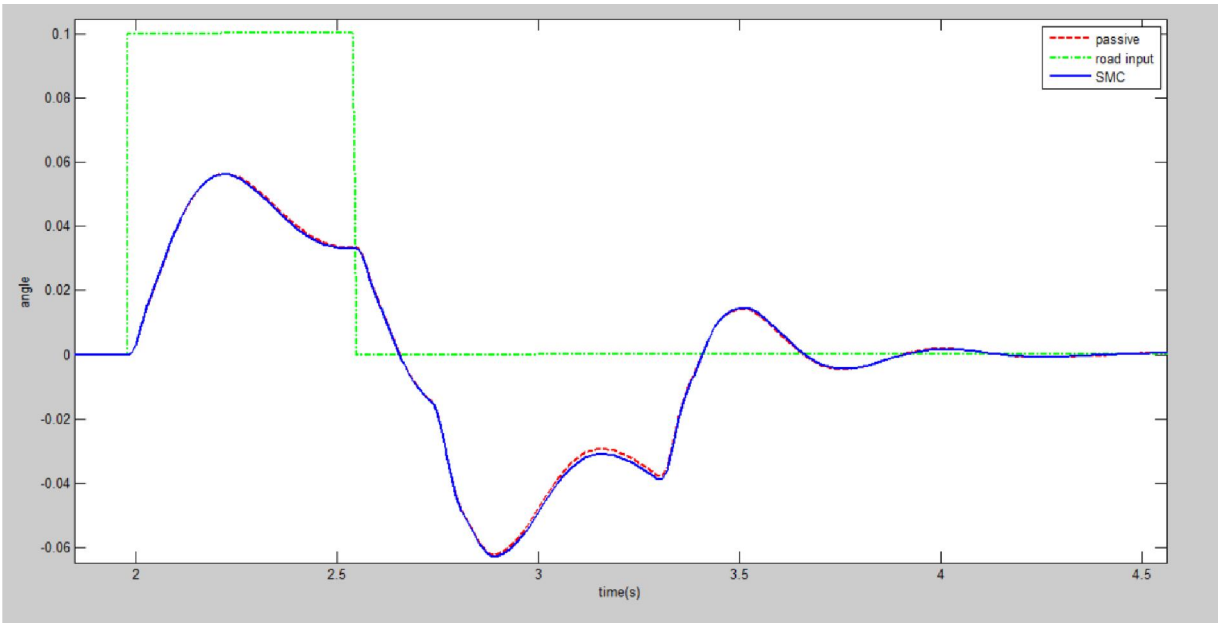

Fig 2.30: Pulse input with amplitude 0.1m and width 0.5s

3.6.3 Step Input

The road input was taken as a pulse with amplitude of 0.1m at time 5s.

Displacement Y (Sprung mass)

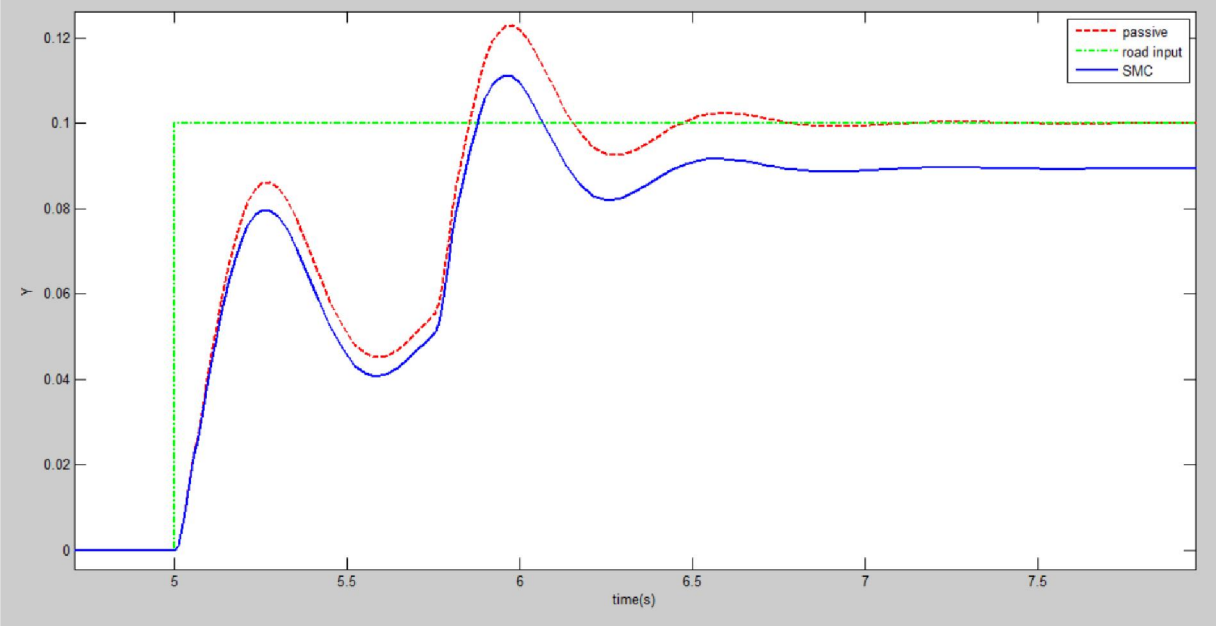

Fig 2.31: Step input-Amplitude 0.1m

From fig 2.31, although both SMC and the passive system have almost the same settling time, the peak value reached by SMC is lesser (0.11m) vs 0.1225m for passive

Displacement between front sprung and unsprung mass (y_1-x_1)

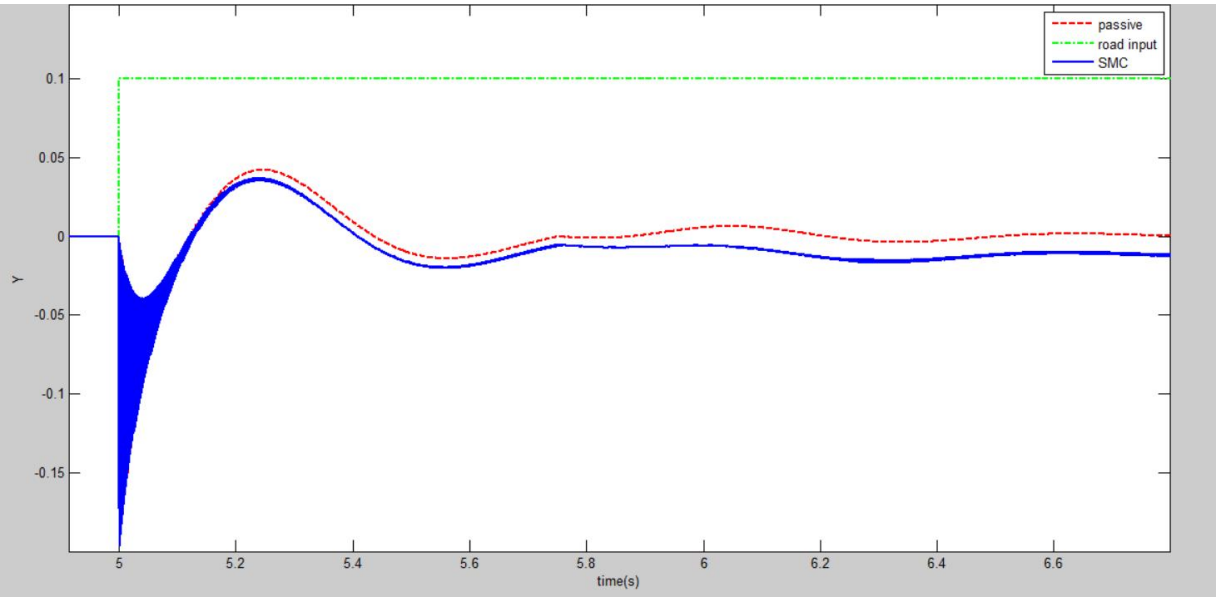

Fig 2.32: Step input-Amplitude 0.1m

Displacement between sprung and unsprung mass(y_2-x_2)

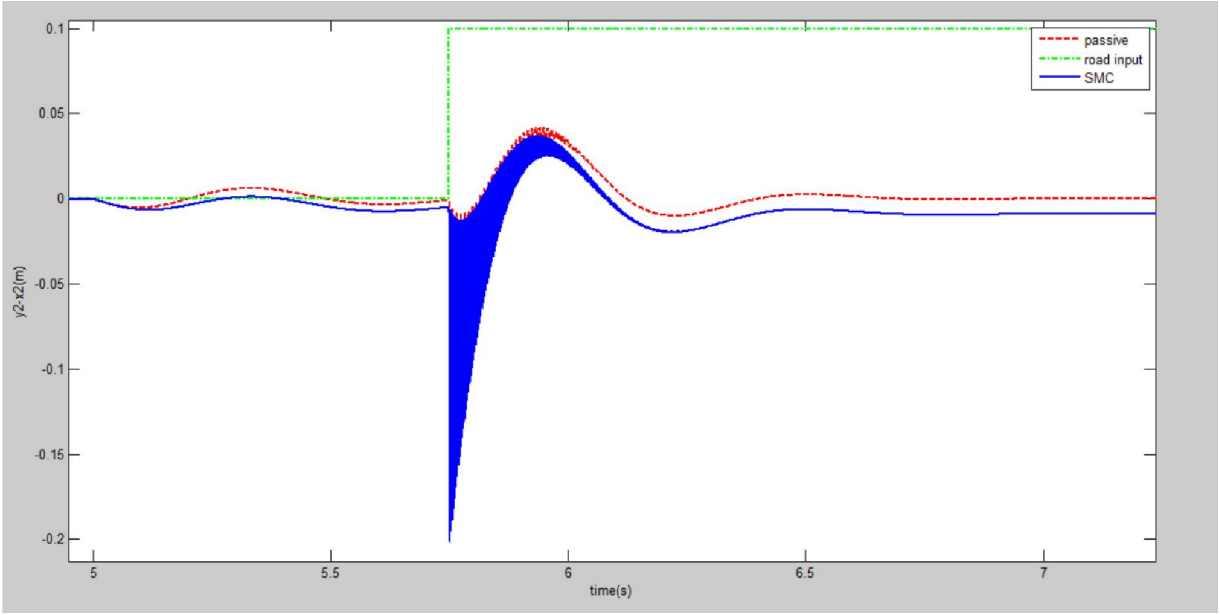

Fig 2.33: Step input-Amplitude 0.1m

Difference between displacement of front unsprung mass and road input(x_1-r_1)

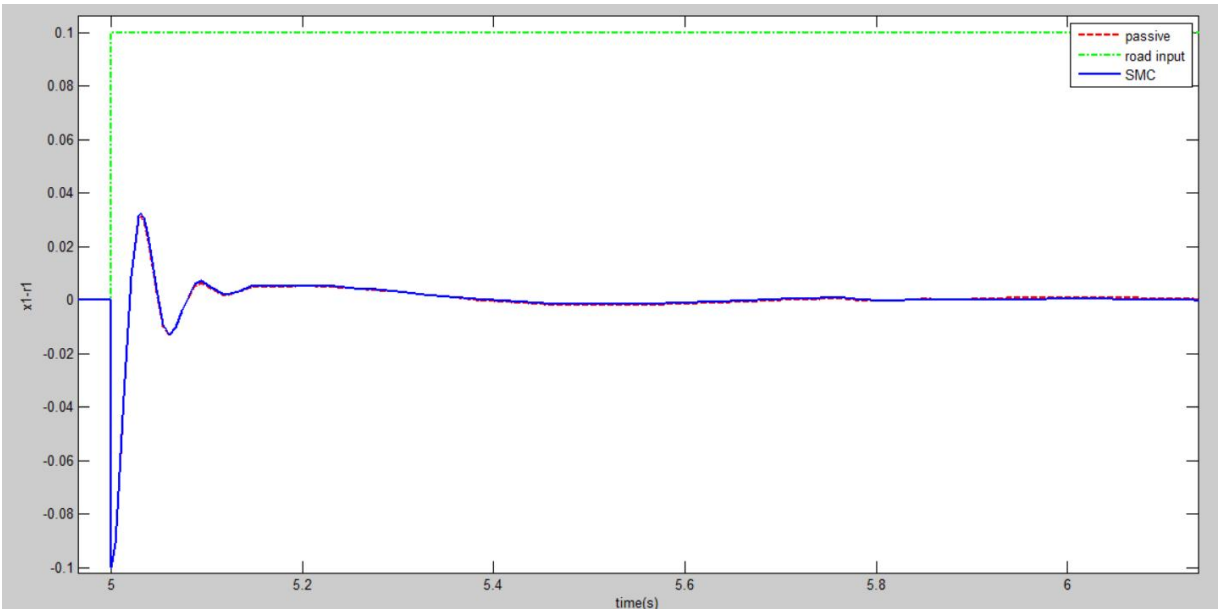

Fig 2.34: Step input-Amplitude 0.1m

Difference between displacement of rear unsprung mass and road input(x_2-r_2)

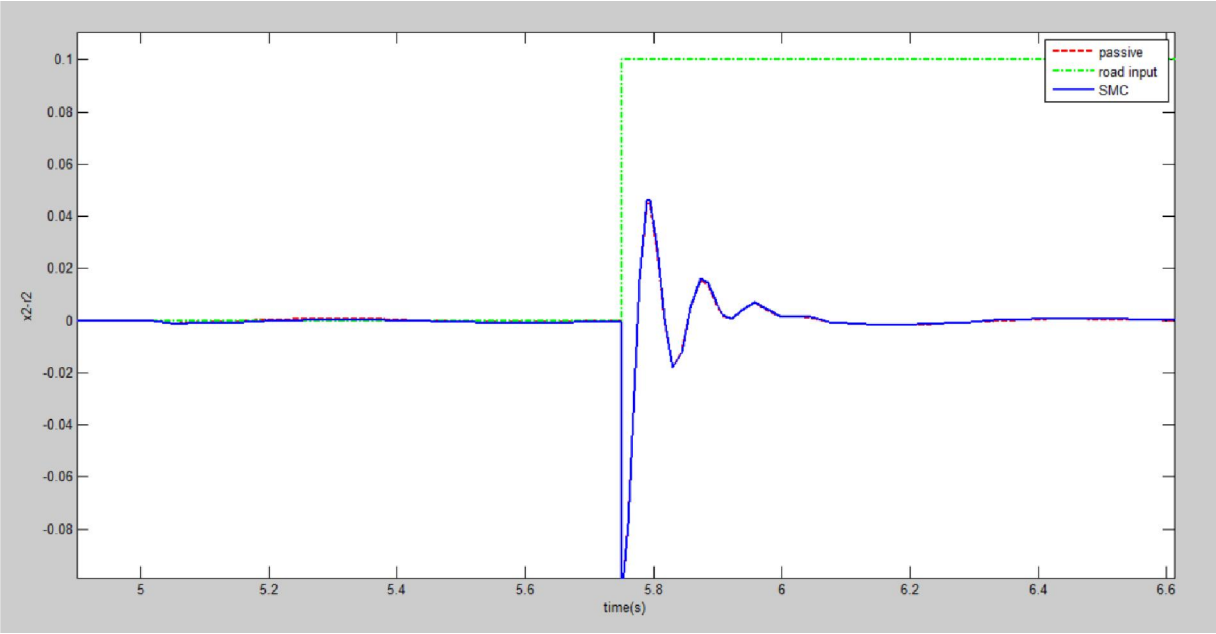

Fig 2.35: Step input-Amplitude 0.1m

Force exerted by controller

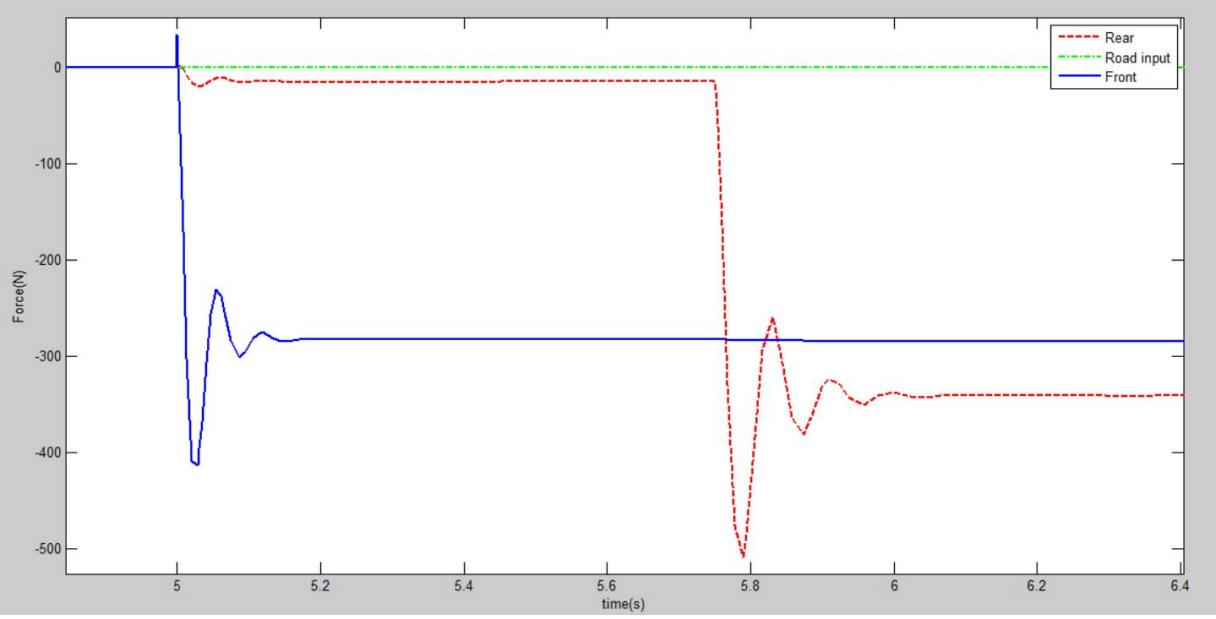

Fig 2.36: Step input-Amplitude 0.1m

From fig 2.36, the rear wheel peaks to a greater negative value(-510N) when compared to the front wheel which peaks to a negative of -412.5N, though the rear wheel has a lag of 0.75 secs.

Pitch

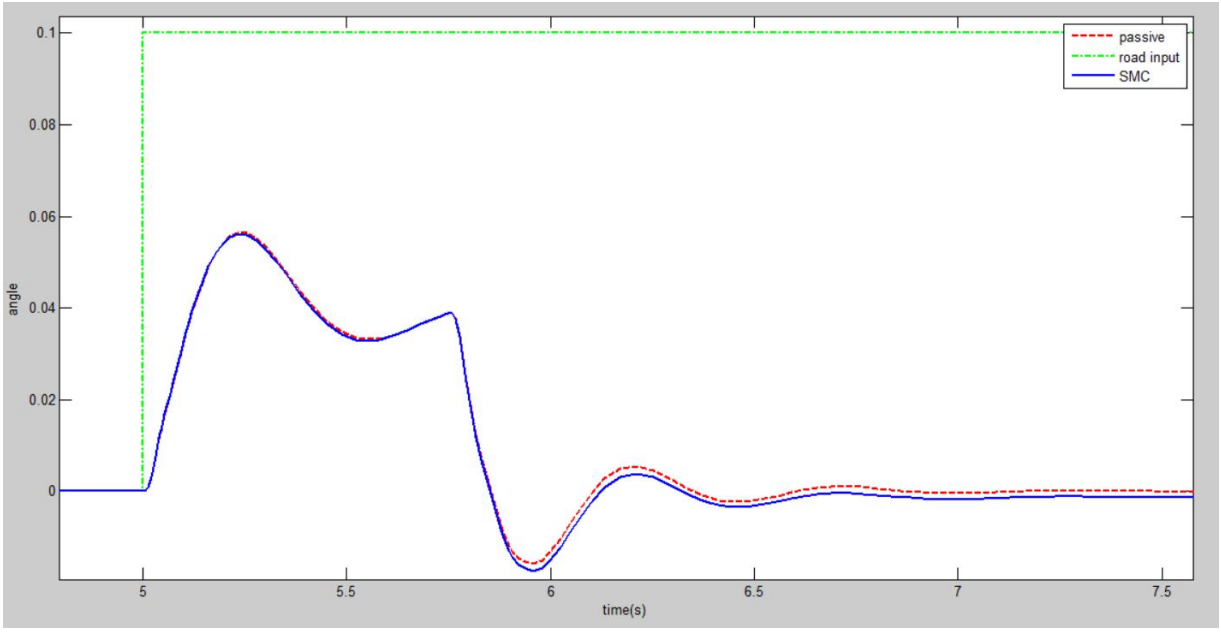

Fig 2.37: Step input-Amplitude 0.1m

CHAPTER 3

3.1 SEMI-ACTIVE SUSPENSION

Semi active suspension systems were first proposed in the early 1970's. In this type of system, the conventional spring element is retained, but the damper is replaced with a controllable dampers. Whereas an active suspension system requires an external energy source to power an actuator that controls the vehicle, a semi active system uses external power only to adjust the damping levels, and operate an embedded controller and a set of sensors. A system with active suspension has the tendency to get easily destabilized, whereas, a desirable system performance can be achieved by the semiactive control system and the stability is more compared to the active system.

3.2 QUARTER CAR MODEL WITH SEMI-ACTIVE SUSPENSION

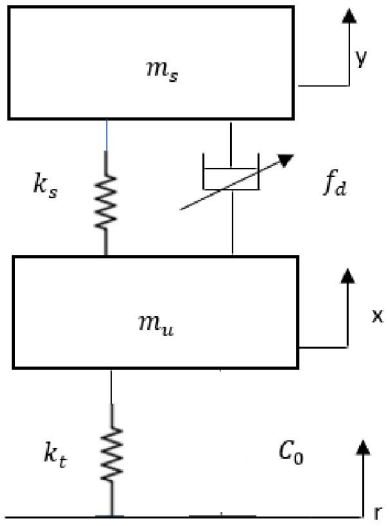

Fig 3.1. Quarter car model with semi-active suspension

PARAMETERS AND NOTATIONS
m_s: mass of car body (sprung mass)
m_u : mass of wheel (unsprung mass)
k_t: spring constant of wheel and tyre
k_s: spring constant of suspension system
f_d : force exerted by the semi-active damper

Based on the equations of the quarter car with passive suspension which were modelled in the first phase of this project, the following equations are arrived at for a semi-active suspension:

$$m_s(\ddot{y}) + k_s(y - x) + f_d = 0$$

$$m_u\ddot{x} - k_s(y - x) - k_t(r - x) - f_d = 0$$

The semi-active damper used here is mathematically Bouc-wen modleled MR damper.

3.3 BOUC-WEN MODEL OF MR DAMPER

A MR damper consists of a hydraulic cylinder, magnetic coils and MR fluid offering design simplicity. In addition to field controllability and design simplicity, MR dampers have many other advantages such as:

(i) They require relatively very low power input,

(ii) Produce high yield stress up to 100 k-Pa,

(iii) Can be stably operated in a wide range of temperature (−40–150 ◦C) and

(iv) MR fluids are not toxic and are insensitive to impurities.

The most extensively used model for modeling hysteretic systems is the Bouc–Wen model. This model contains components viscous damper, spring and a hysteretic component. The MR damper with Bouc-Wen model is composed of stiffness (spring) element passive damper and Bouc-Wen hysteresis loop elements. The schematic representation of the Bouc-Wen model of an MR damper is represented in Fig. 3.2, where Z is the displacement from the rest position, K_0 is the stiffness coefficient, C_0 is minimum damping coefficient, f_0 is the pre-yield stress.

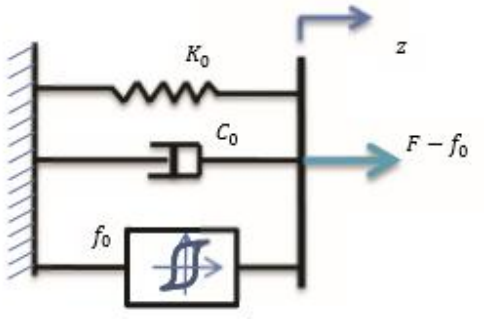

Fig 3.2. Schematic Representation of Bouc – Wen model of an MR damper

The model equation of the Bouc – Wen model is represented as follows:

$$\dot{y_1} = -\gamma\,|\dot{z}|\,y_1\,|\,y_1|^{n-1} - \beta\,z\,|\,y_1|^n + A\dot{z}$$

y_1 is an evolutionary variable that can vary from a rectangular to a quasi-rectangular function of time depending on the parameters γ, β and A.

The force exerted by the MR damper is the function of the relative displacement z and velocity and the parameter α defined by the control voltage u, and is given by:

$$F_{mr} = C_0\,(u)\,\dot{z} + K_0\,z + \alpha\,(u)\,y_1 + f_0$$

In the above equation, K_o stands for the stiffness of the spring element of the MR damper. C_o (u) and α (u) have a linear relationship with control voltage V. The force f_o is the pre yield stress of the damper.

$$C_0\,(u) = C_{0a} + C_{ob}\,V$$

$$\alpha\,(u) = \alpha_{0\alpha} + \alpha_{0b}\,V$$

Where V is given by:

$$\dot{V} = -\eta(V - v)$$

v is the voltage applied to the damper and η is a constant governing the rate of change of magnetic field to reach the equilibrium of the MR fluid.

3.4. SUSPENSION SYSTEM CONTROLLER

Deriving the Control Law

In this controller, the ideal skyhook is used as a reference model and the sliding mode control technique is used to force the system sprung mass motion to track the sprung mass motion of the reference model. Since it is a second order system, equation of the sliding surface becomes:

$S = \dot{e} + \lambda e$ (1)

Where $e = y - y_{ref}$ (2)

The sliding condition must be defined to ensure that the states will move toward and reach the sliding surface.

Sliding condition: $(\frac{1}{2})(\frac{dS^2}{dt}) \leq |S|$

Or $S\dot{S} \leq -|S|$ (3)

Differentiating equation (1),

$\dot{S} = \ddot{e} + \lambda\dot{e}$ (4)

From the above equations and the equations of the quarter car model,

$\dot{s} = \frac{-K_s}{m_s}(y - x) - \frac{f_d}{m_s} - \ddot{y_{ref}} + \lambda\dot{e}$ (5)

Putting $\dot{s} = 0$,

$f_{d0} = -k_s(y - x) - m_s(\ddot{yref}) + m_s(\lambda)(\dot{y} - \dot{yref})$ (6)

Thus, to account for the mass uncertainty while satisfying the sliding condition a term discontinuous across the surface is added to the f_{d0} then take the control law or the desired damping force as:

$\boxed{f_c = f_{d0} - (k_d)sgn(S)}$ (7)

Where sgn is the surface function sign and k_d is a switching gain. Hence, using Equation (7), the system trajectory will take finite time to reach the surface $S(t)$, after which the error will exponentially go to zero.

An ideal sliding mode exists only when the state trajectory $x(t)$ of the controlled plant agrees with the desired trajectory at every time. To avoid chattering effect,

$$f_c = \begin{cases} f_{d0} - K_d s \; if \; |S| \leq 1 \\ f_{d0} - K_d sgn(s) if \; |S| > 1 \end{cases} \quad (8)$$

Now considering $\dot{V_{SMC}} = s\dot{s}$,

To guarantee that the system state asymptotically switches to the sliding surface, it is defined that,

$$\dot{V_{SMC}} = S\dot{S} \leq -\phi|S| \quad (9)$$

Where ϕ is a positive constant.

$$\ddot{y}=\frac{1}{m_s}[(-k_s)(y-x)-f_d] \quad (10)$$

Combining (11) & (20),

$$\dot{S}=\frac{1}{m_s}[(-k_s)(y-x)-f_d]-\ddot{y_{ref}}+\lambda\dot{e} \quad (11)$$

Using f_c to replace f_d in equation (11),

$$\dot{V_{SMC}}=(-\frac{k_s}{m_s}(y)+\frac{k_s}{m_s}(\mathrm{x})-\frac{f_c}{m_s}-\ddot{y_{ref}}+\lambda\dot{e})\,\mathrm{S} \quad (12)$$

Substituting (7) in (12) and combining with (6) we get,

$$\dot{V_{SMC}} = [(\frac{1}{m_s}-\frac{1}{m_{s0}})(-k_s y + k_s x - f_{d0} + \frac{k_d}{m_s}sgn(s)]s \quad (13)$$

According to the Lyapunov stability condition of SMC, substituting equation (13) in (9) and considering $|s| = s.sgn(s)$,

$$\left[\left(\frac{1}{m_s}-\frac{1}{m_{s0}}\right)(-K_s y + K_s x - f_{d0}) + \frac{k}{m_s}sgn(s)\right]s \leq -\phi.s.sgn(s) \quad (14)$$

For s≥ 0, (24) is simplified as:

$$k_d \leq -m_s\phi + (1-\frac{m_s}{m_{s0}})(k_s\mathrm{y} - k_s\mathrm{x} + f_{d0}) \quad (15)$$

And for $s < 0$, then,

$$k_d \leq -m_s\phi + \left(1 - \frac{m_s}{m_{s0}}\right)(-k_s y + k_s x - f_{d0}) \quad (16)$$

Considering that the real load of a vehicle is often variable, we define q as the variation rate of vehicle sprung mass to its empty load sprung mass m_{s0}, i.e., $q = \frac{m_s}{m_{s0}} \geq 1$

$$\boxed{k_d = -m_{s0}q\phi - (q-1)(|f_{d0}| + k_s|y| + k_s|x|)} \quad (17)$$

Damper Control Strategy

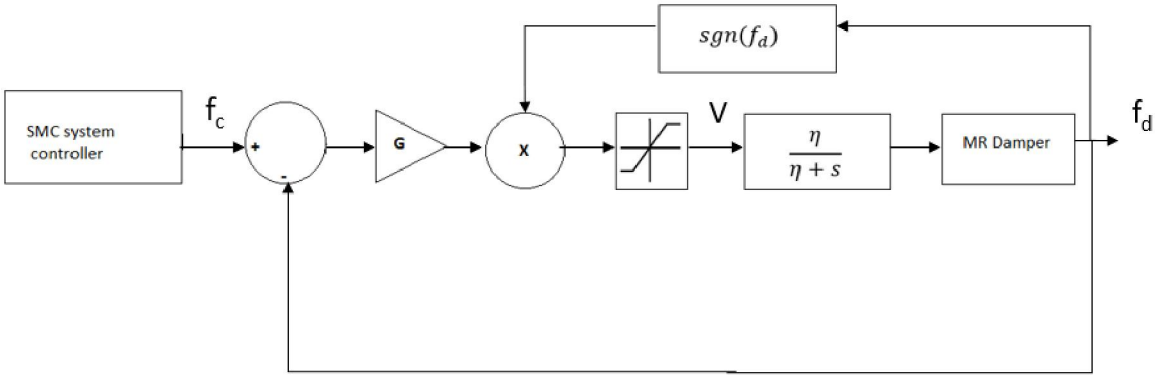

Fig 3.3. Block diagram of the damper SMC controller

As shown the MR damper damping force f_d is a feedback signal compared to the system desired force f_c which was calculated based on the sliding mode control and reference model. To guarantee that the control signal sent to the damper is not to generate energy, the control function is enabled only when the direction of the desired damping force and the error having the same direction. If the control function and the desired force have different sign, then the damper input voltage is set to zero.

$$v = G(f_c - f_d)sgn(f_d)$$

If $G(f_c - f_d)sgn(f_d) > V_{max}, then\ v = V_{max}$

If $G(f_c - f_d)sgn(f_d) < V_{min}, then\ v = V_{min}$

where
$V_{max}$is the MR damper saturation voltage (2 volt),
$V_{min}$is the MR damper minimum voltage (zero volt),
$f_c$is the suspension desired damping force,
$f_d$is the MR damper actual force,
$G$is a scaled gain.

3.5. SIMULINK MODEL OF QUARTER CAR WITH SMC CONTROLLED SEMI-ACTIVE SUSPENSION

Fig 3.4. (a) Bouc-wen model

Fig 3.4. (b) Modelling of f_{d0} and K_d 's equations

Fig 3.4. (c) Modelling of f_c and Sliding surface's equations

Fig 3.4. (d) MR Damper controller

Fig 3.4. (e) Full Block diagram of the SMC controlled quarter car with semi-active suspension

3.6. SIMULATION RESULTS AND ANALYSIS

The Simulink Model shown in section 3.5 was used to test the various parameters of the quarter car with SMC controlled semi-active suspension for different road inputs namely Sine wave, step and pulse input. The same were recorded for a quarter car with passive suspension in order to compare. These parameters are displacement and acceleration of sprung mass, difference in displacements of sprung and unsprung masses, and that of unsprung mass and road input. The force exerted by the Bouc-Wen model of the damper was also recorded in each case.

3.6.1. Sine Wave Road Input

The road input was taken as sine wave with amplitude of 0.1m and frequency was varied from 0.1 Hz to 20 Hz.

Displacement of Sprung mass (y)

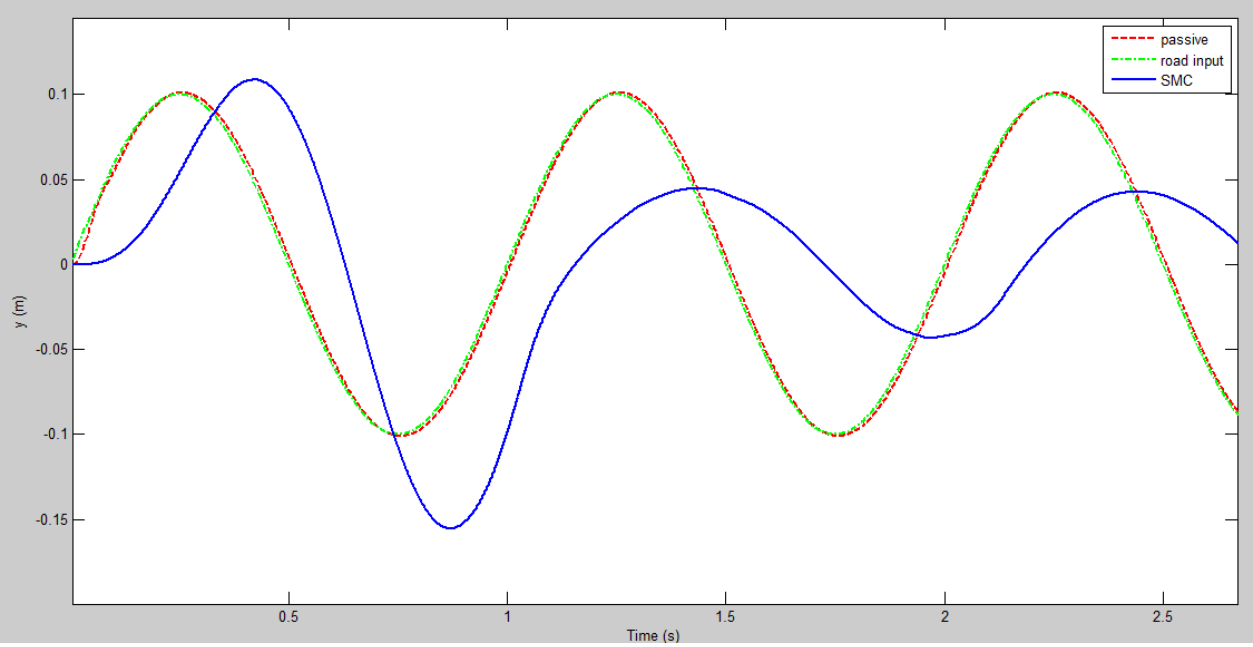

Fig 3.5: Input: Sine wave (0.1 m, 1Hz)

Figure 3.5 illustrates the response of SMC compared with Passive system when excited with a road input of Sine Wave of amplitude = 0.1 m and a frequency = 1Hz. Although the overshoot of SMC system is slightly higher than the passive system on both the positive and negative fronts, i.e., 0.108m and -0.150m as compared to 0.1m and -0.1m, the former settles as a sine wave of amplitude 0.044m after one cycle of overshoot, i.e. 1.15s, itself. However, the passive system's output doesn't. Also, there's a phase shift of approximately 90 degrees in case of SMC.

Sine waves with varied frequencies were analyzed for the displacement of sprung mass. These have been illustrated in the Figures 3.6-3.8.

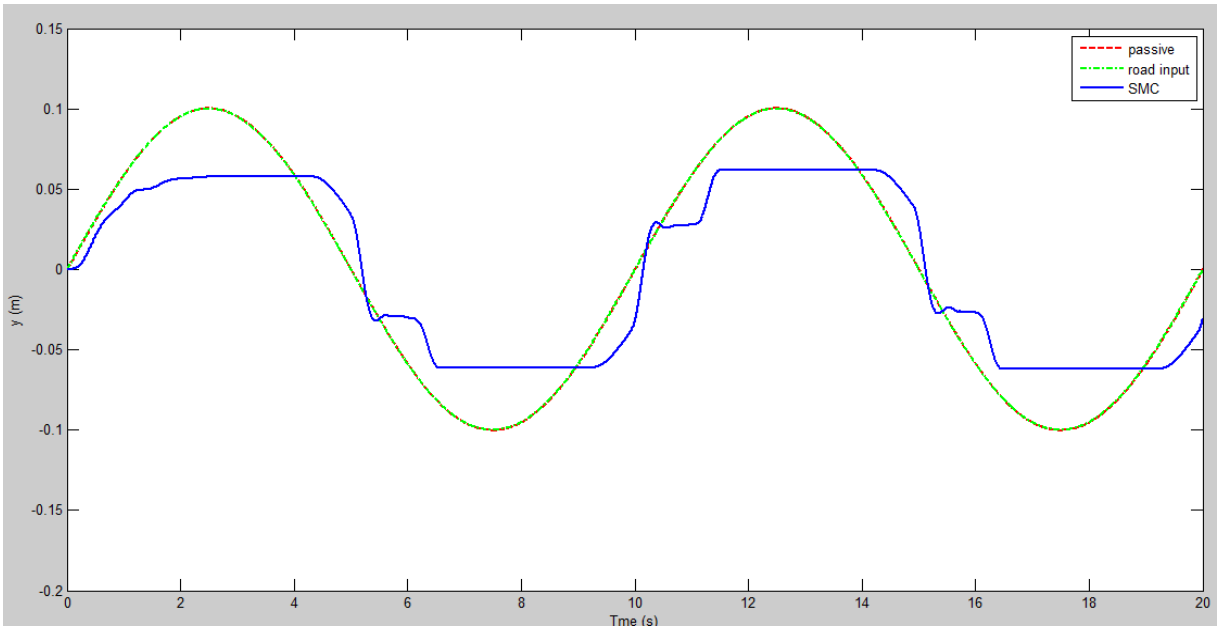

Fig 3.6: Input: Sine wave (0.1 m, 0.1Hz)

The maximum overshoot of y for the SMC system here is lower than passive, i.e. 0.058m. The phase shift and settling time has notable reduced however, with the presence of some distortions.

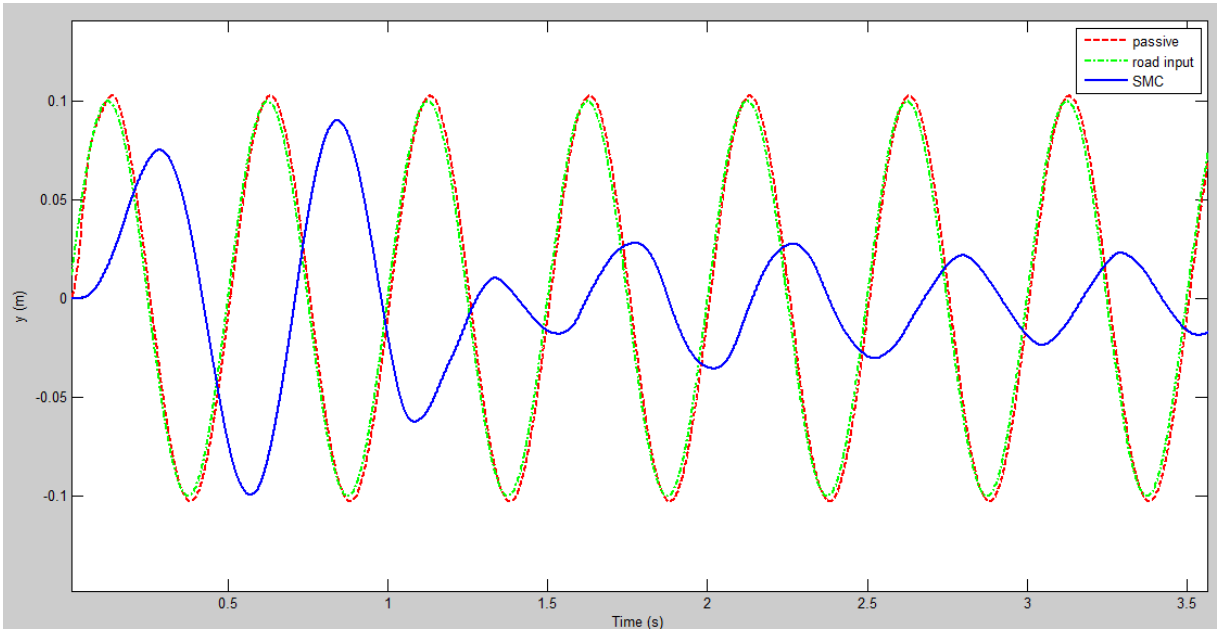

Fig 3.7: Input: Sine wave (0.1 m, 2Hz)

In Fig. 3.7, the overshoot is 0.0905 and -0.0993 which settles in 2.795s to a sine wave of 0.0207 amplitude. The phase shift is lesser than 90 degrees as was for frequency of 1 Hz.

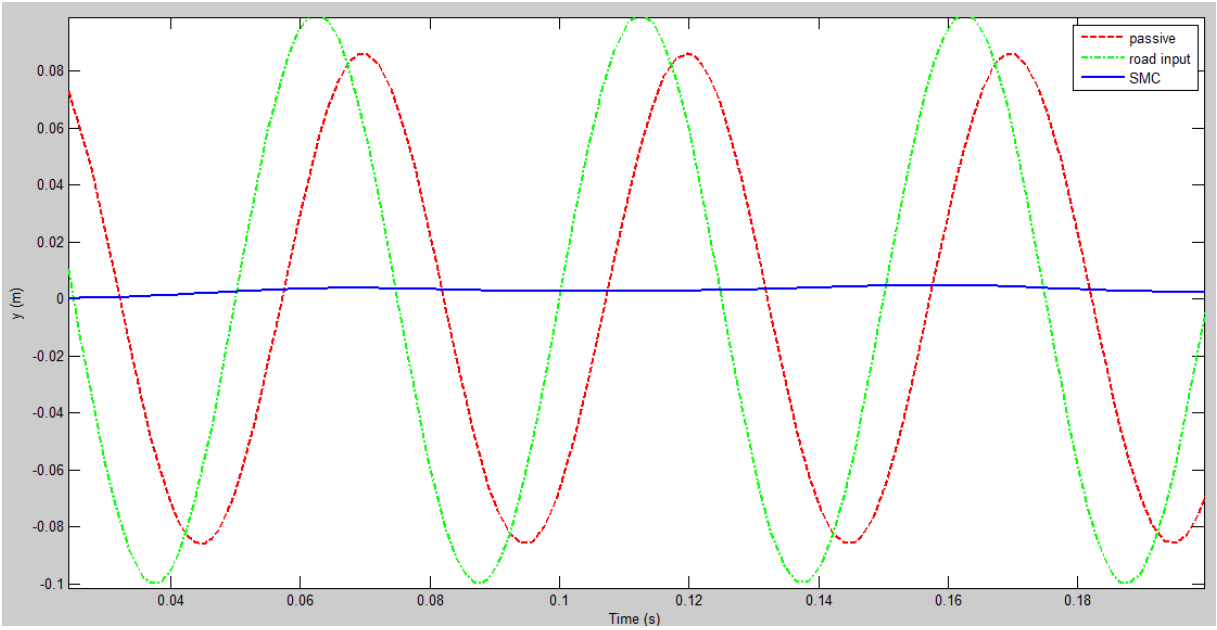

Fig 3.8: Input: Sine wave (0.1 m, 20Hz)

In Fig. 3.8, the overshoot is 0.0048 which settles in approximately the same time 2.79s as 2Hz. Here, a reduction in amplitude of output of passive system is also seen.
It is noted that the overshoot of the displacement of sprung mass is reducing for increasing frequencies and the settling time is approximately the same (as seen for frequencies between 1Hz and 20Hz). The phase shift reduces for the increasing frequencies too.

Vertical acceleration of Sprung mass (ÿ)
Besides the displacement of sprung mass, the vertical acceleration of the same also plays an important role in determining the extent of road comfort of a vehicle.

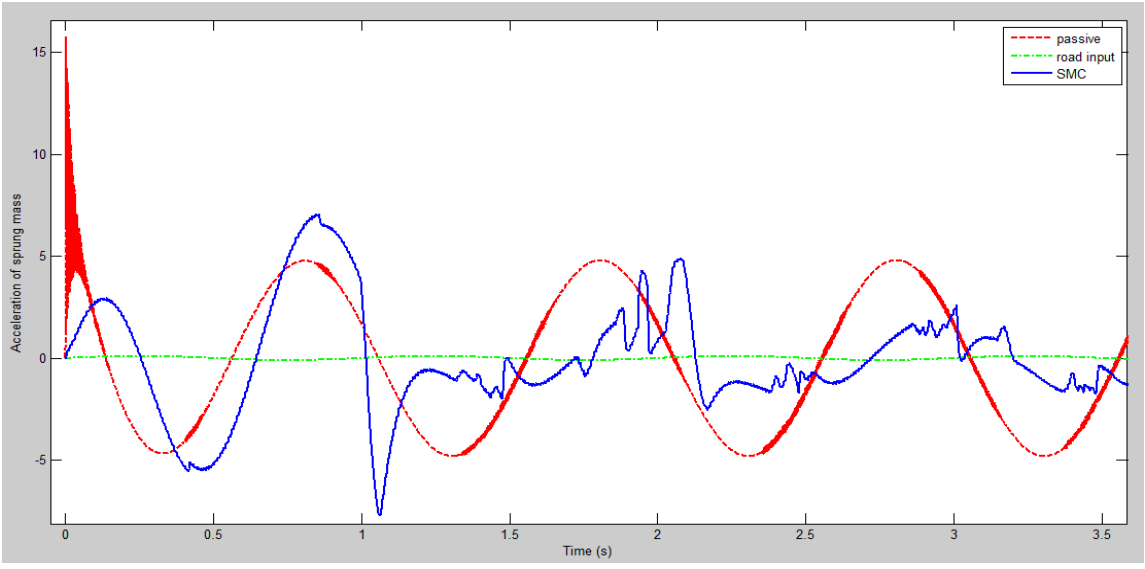

Fig 3.9: Input: Sine wave (0.1 m, 1Hz)

Figure 3.9 illustrates the vertical acceleration of sprung mass (m/s^2) of SMC compared with Passive system when excited with a road input of Sine Wave of amplitude = 0.1 m and a frequency = 1Hz. The maximum overshoot of SMC system is 7.09 m/s^2 which in 3.56 seconds comes down to non-sinusoidal oscillations of maximum amplitude 1.8 m/s^2. This is desirably low from the passive system that records a maximum overshoot of 15.76 m/s^2 that settles to sine wave of amplitude 4.75 m/s^2.
Sine waves with varied frequencies were analyzed for the acceleration of sprung mass. These have been illustrated in the Figures 3.10-3.13.

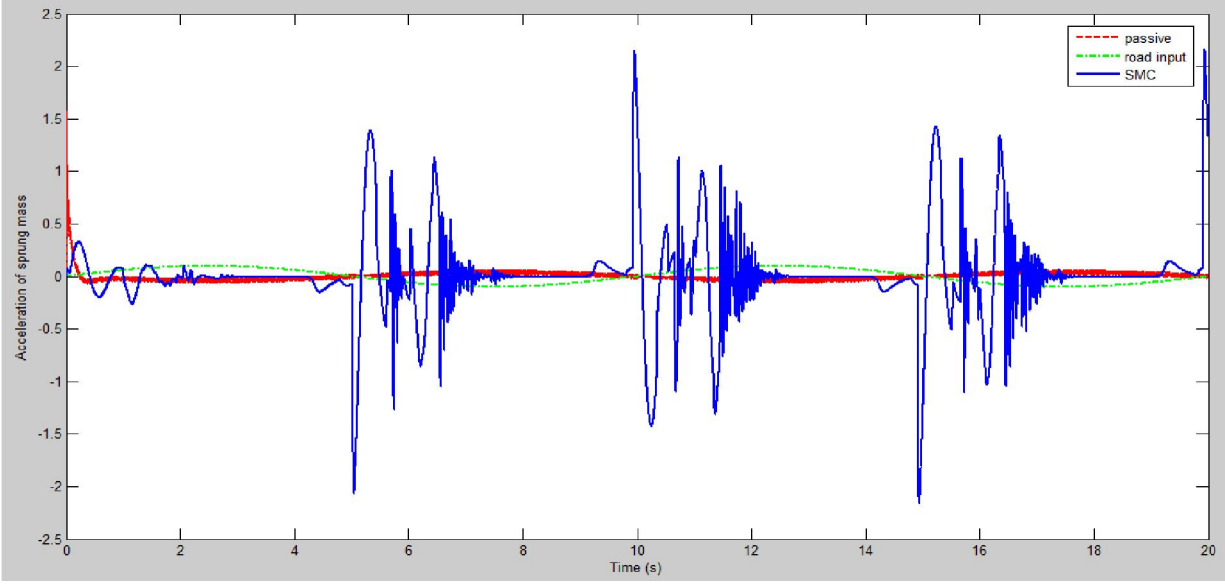

Fig 3.10: Input: Sine wave (0.1 m, 0.1Hz)

In Figure 3.10, the maximum overshoot of SMC system is 2.154 m/s^2 when compared to 1.576 m/s^2 of passive system. The SMC controller gives undesirable vertical acceleration of sprung mass at lower frequencies. Also, an overshoot is seen at each zero crossing of the road input which takes 50% of the time till next zero-crossing to settle.

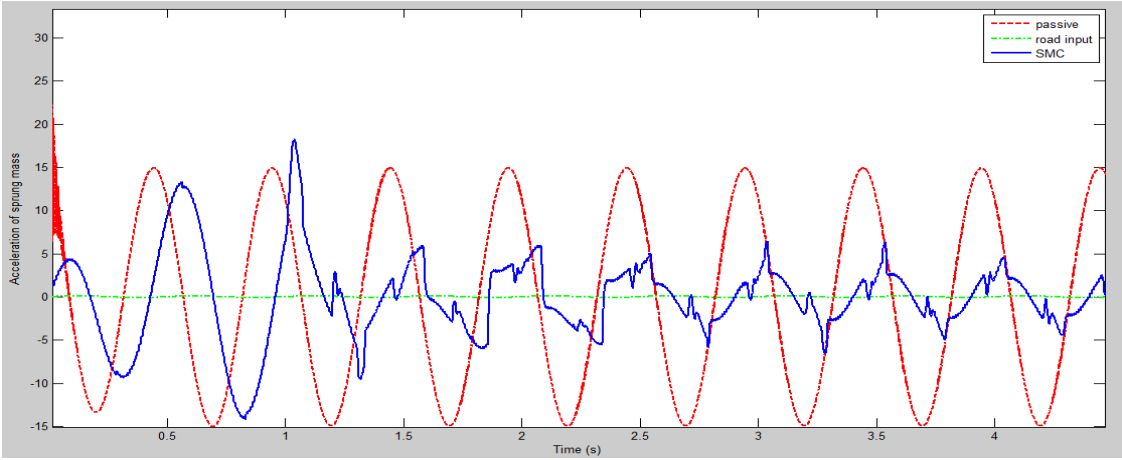

Fig 3.11: Input: Sine wave (0.1 m, 2Hz)

In Fig. 3.11, the maximum overshoot of SMC system is 18.25 m/s^2 which in 3.81 seconds comes down to non-sinusoidal oscillations of maximum amplitude 4.98 m/s^2. This is lower than the passive system that records a maximum overshoot of 31.51 m/s^2 that settles to sine wave of amplitude 14.92 m/s^2.

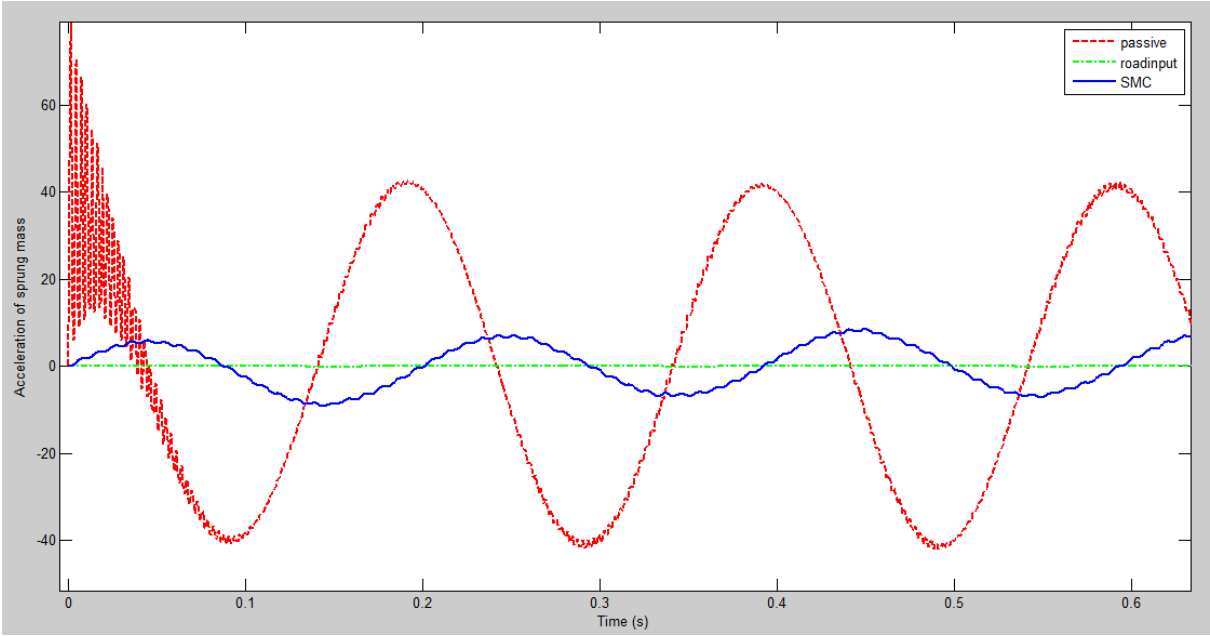

Fig 3.12: Input: Sine wave (0.1 m, 5Hz)

In Fig. 3.12, the maximum overshoot of SMC system is 9.2 m/s^2 which in 1.169 seconds comes down to non-sinusoidal oscillations of maximum amplitude 6.84 m/s^2.

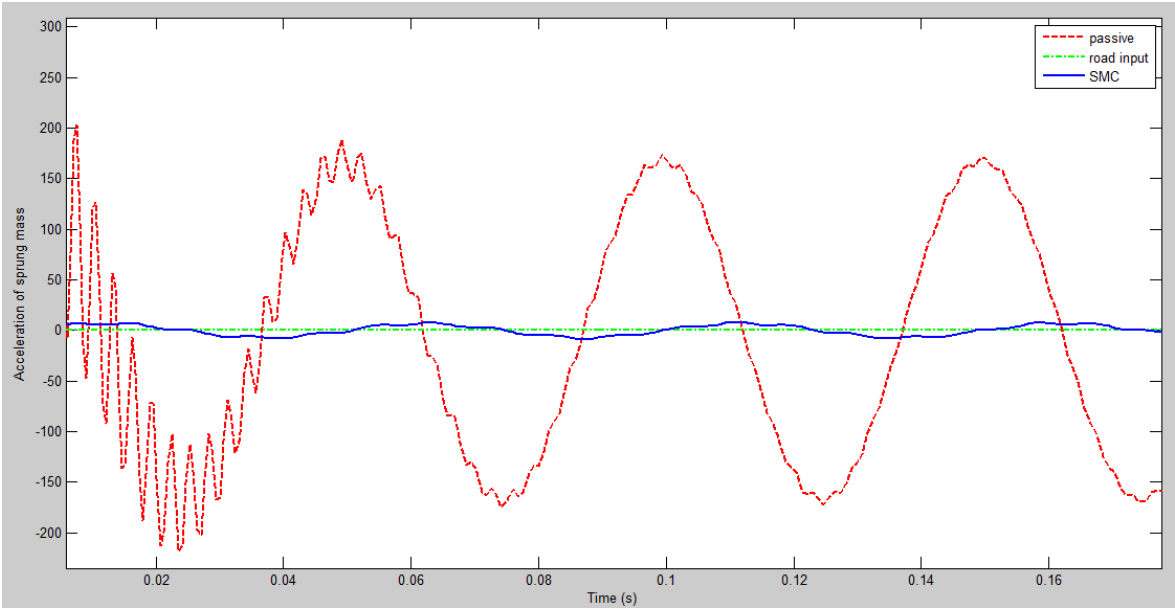

Fig 3.13: Input: Sine wave (0.1 m, 20Hz)

In Fig. 3.13, the maximum overshoot of SMC system as seen has reduced considerably to 8.2 m/s^2. From the values noted from the above figures (3.10-3.13), it is seen that the vertical accelerations of sprung mass in SMC controlled system increase with increasing frequency till a certain frequency (here, between 2 to 5 Hz) and then begin to reduce. The same trend is seen for the settling time. In case of passive suspension, the accelerations continuously increase with frequency. Also, initially, they vary at a very high rate before settling at a sine wave of lower amplitude. This behavior can be seen clearly in the figure 3.12 and 3.13.

Difference in displacements of sprung and unsprung mass (y-x)

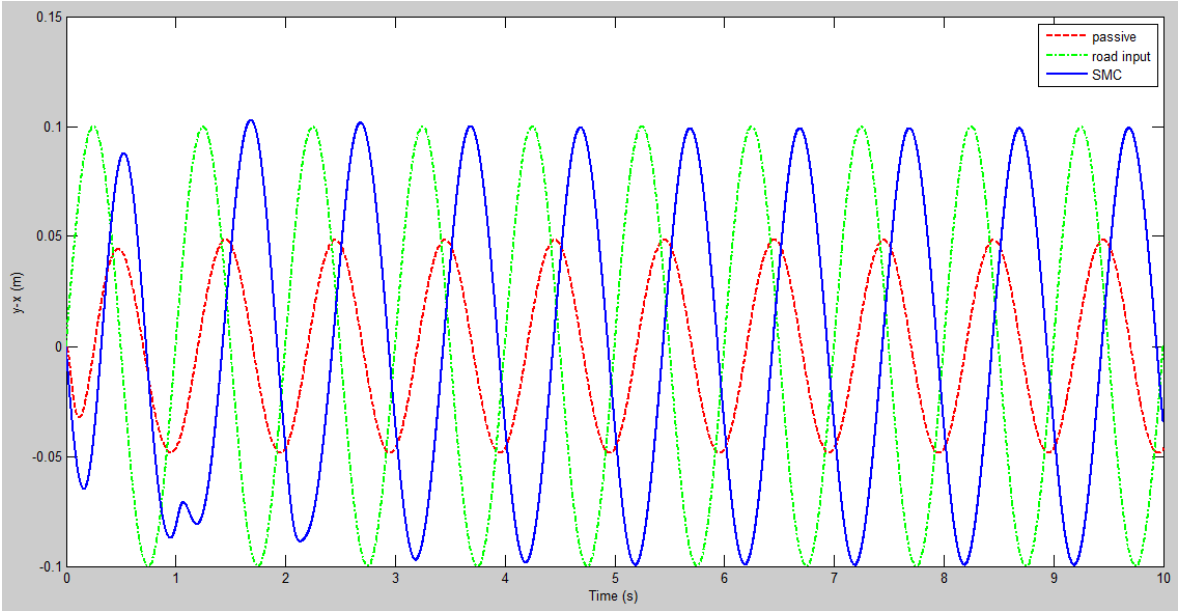

Fig 3.14: Input: Sine wave (0.1 m, 1Hz)

Figure 3.14 illustrates the difference between displacements of sprung and unsprung mass (m) of SMC compared with Passive system when excited with a road input of Sine Wave of amplitude = 0.1 m and a frequency = 1Hz. The amplitude of SMC system is 0.1m and that of passive system is 0.0485m. This difference in both the outputs is not undesirable. The higher value in case of SMC only denotes that the sprung and unsprung mass does not deflect in the same direction and hence, the difference in signs reflects here.

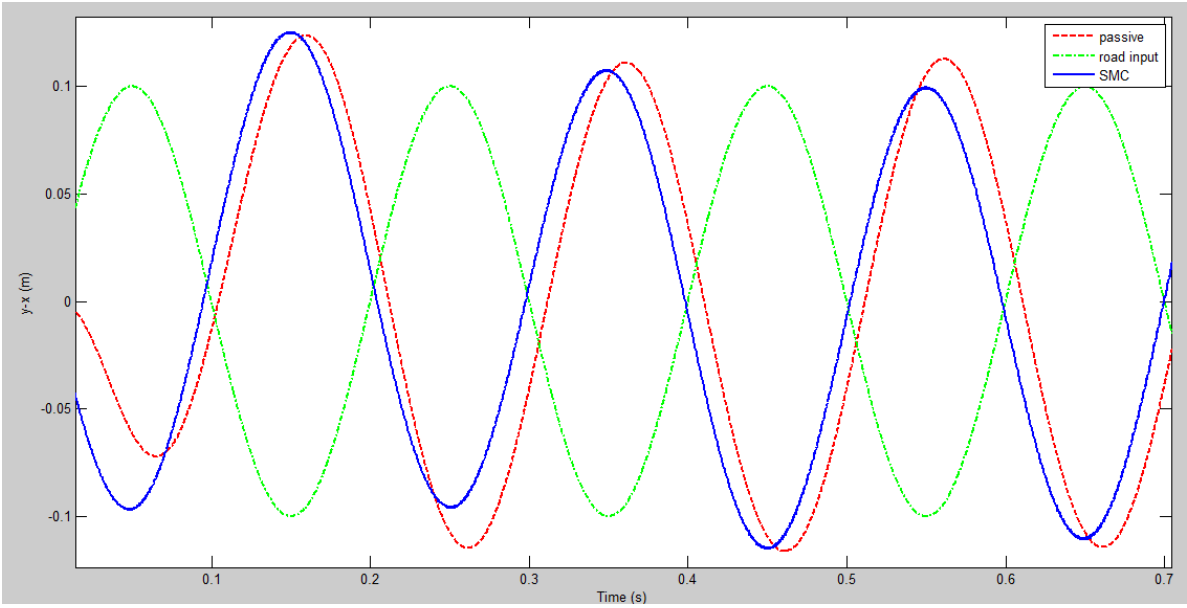

Fig 3.15: Input: Sine wave (0.1 m, 5Hz)

In Figure 3.15 both, the SMC and passive system see deflection of sprung and unsprung masses in opposite directions. Hence, the difference in SMC system is initially 0.1255m which drops to a sine wave of 0.106m amplitude, and that in case of passive varies from 0.123m to 0.1136m. The amplitude of former is desirably lower than the latter.

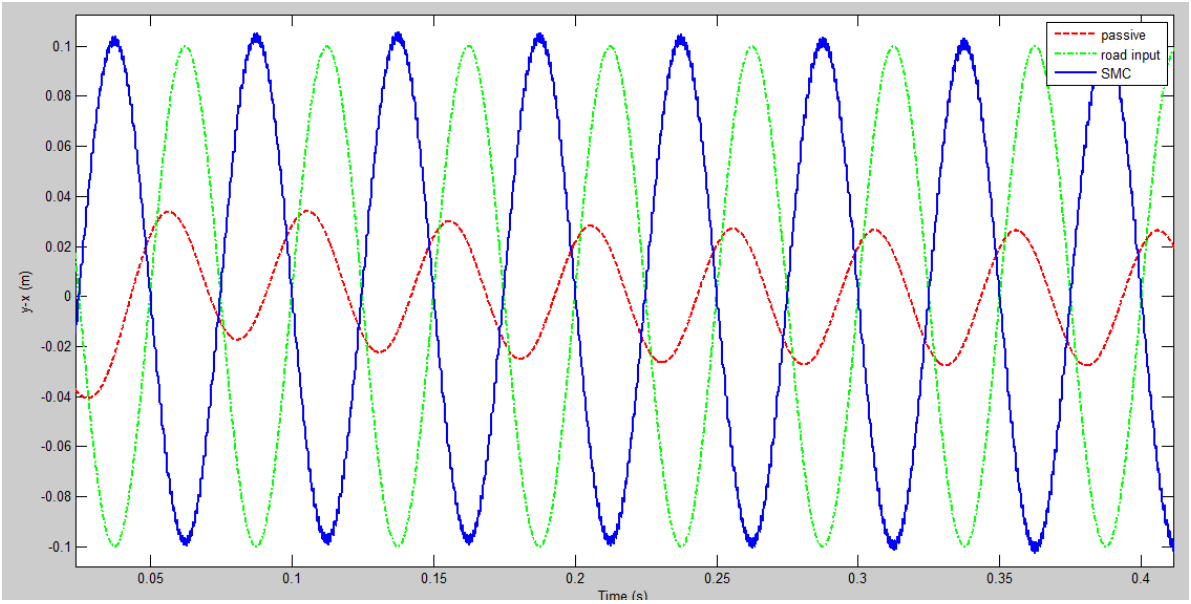

Fig 3.16: Input: Sine wave (0.1 m, 20Hz)

In Figure 3.16, again the behavior is similar to when the frequency was 1 Hz, i.e., deflection in opposite directions in case of SMC alone. The value of amplitudes of the sine waves in SMC and passive systems are 0.105m and 0.027m respectively.

It is seen that in SMC controlled semi-active damper system, the deflection of sprung and unsprung mass is always in opposite direction. This causes a slight phase shift and reflects the small delay in response of displacement of sprung mass as compared to unsprung mass.

Difference in displacements of unsprung mass and road input (x-r)

The aim of the SMC controller was to increase road comfort by reducing the deflection of the sprung mass. However, the same has an effect on the road handling too which is reflected by the difference in displacements of unsprung mass and the road input. The same is studied for sine waves of three different frequencies in the figures 3.17-3.19.

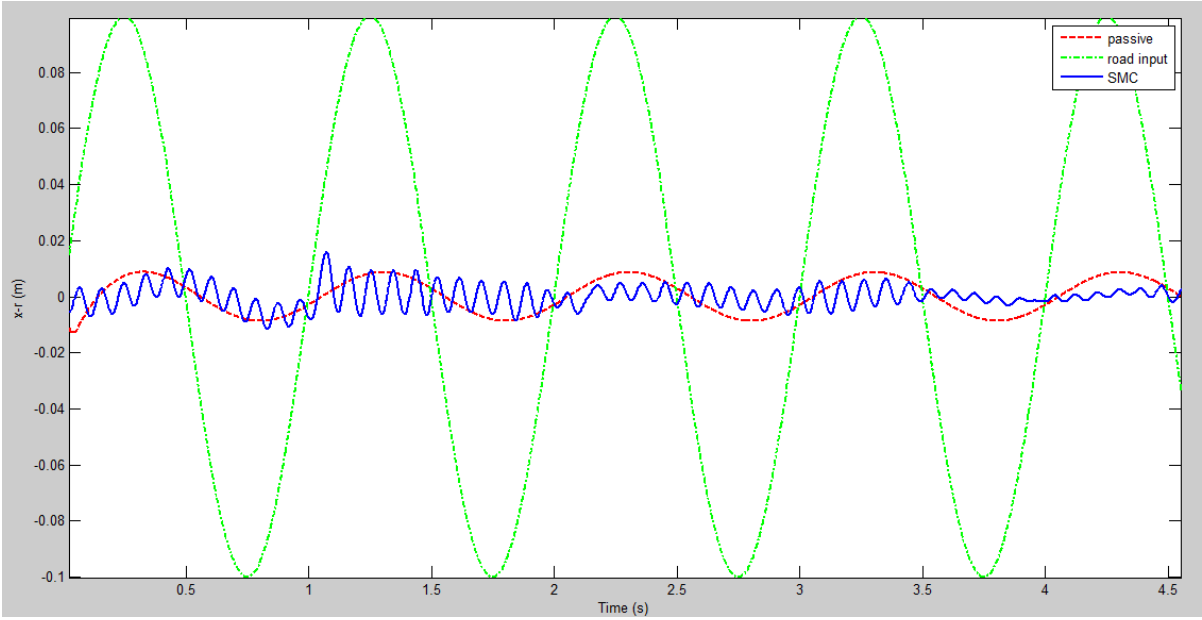

Fig 3.17: Input: Sine wave (0.1 m, 1Hz)

In Fig. 3.17, the difference x-r (displacement of unsprung mass- road input) is seen to be a sine wave for passive system with an amplitude of 0.0087m, where as for SMC, the maximum overshoot is 0.0159m. The settling time is 3.99s, after which it is a sine wave of 0.0023m amplitude which is clearly lesser than the passive case.

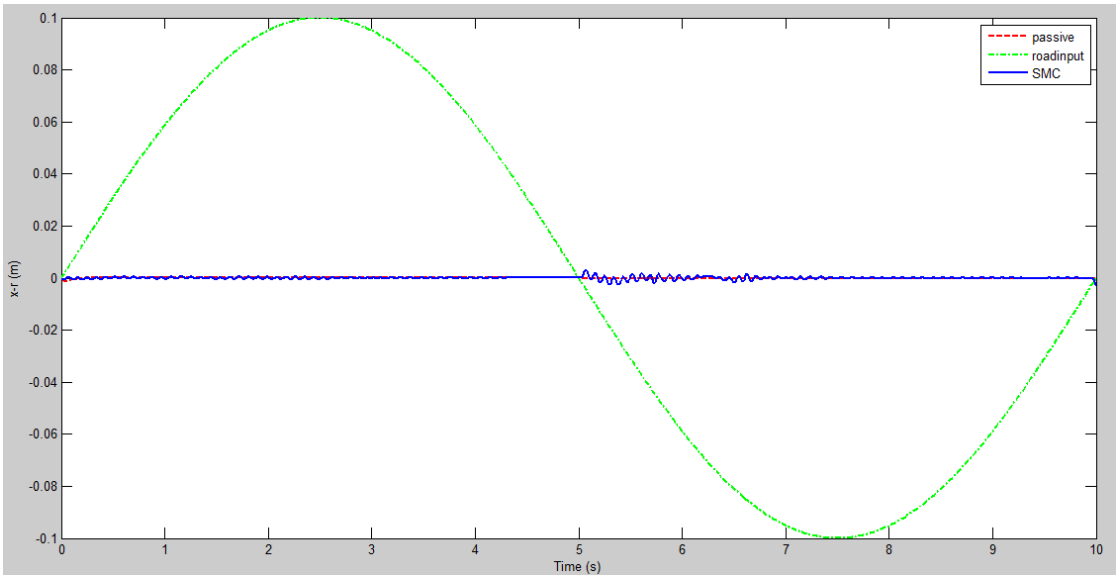

Fig 3.18: Input: Sine wave (0.1 m, 0.1Hz)

In Fig. 3.18, the difference x-r is almost zero for passive system, where as for SMC, the amplitude is 0.0032m.

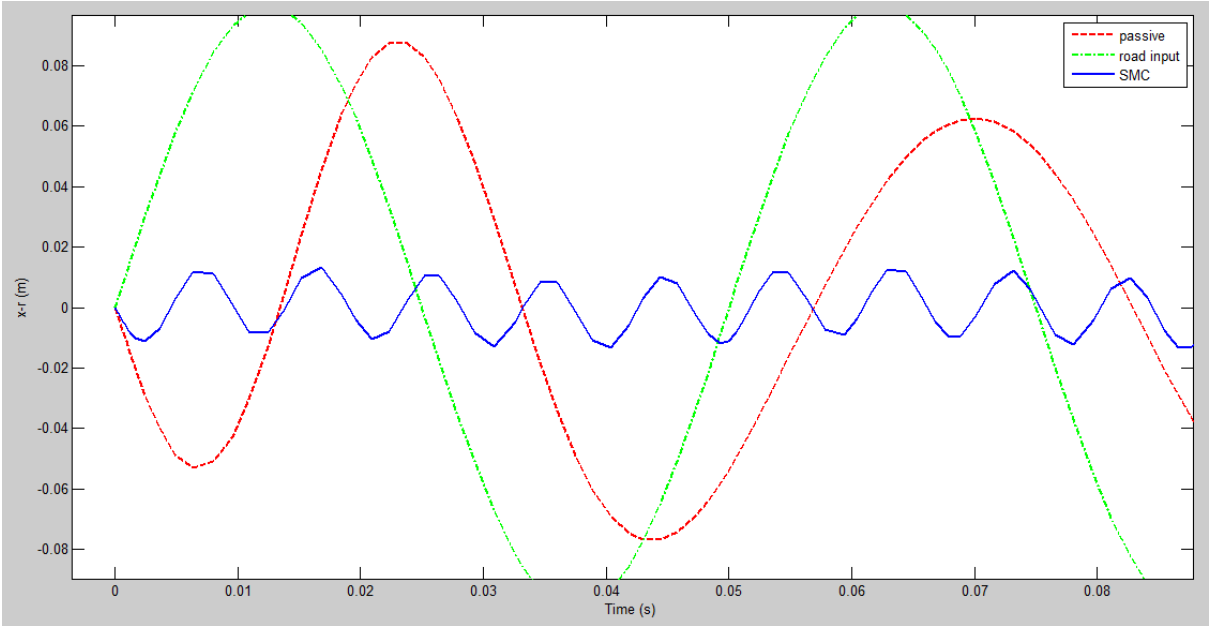

Fig 3.19: Input: Sine wave (0.1 m, 20Hz)

In Fig. 3.19, the difference x-r is seen to be a sine wave for passive system with an amplitude of 0.066m, where as for SMC, it is 0.0128m. It is seen that the road handling for a passive system reduces with increase in frequency (increasing amplitude of x-r) and in case of SMC controlled semi-active suspension system, the road handling has desirable characteristics in a range of frequencies only, as here, the amplitude of x-r increase for 20Hz sine wave although it reduced in case of 0.1 Hz to 1Hz.

Force exerted by the damper that is based on Bouc-wen model (N)

Figures 3.20 and 3.21 illustrate the force exerted by the semi-active damper with respect to time for frequencies 1 and 0.1 Hz.

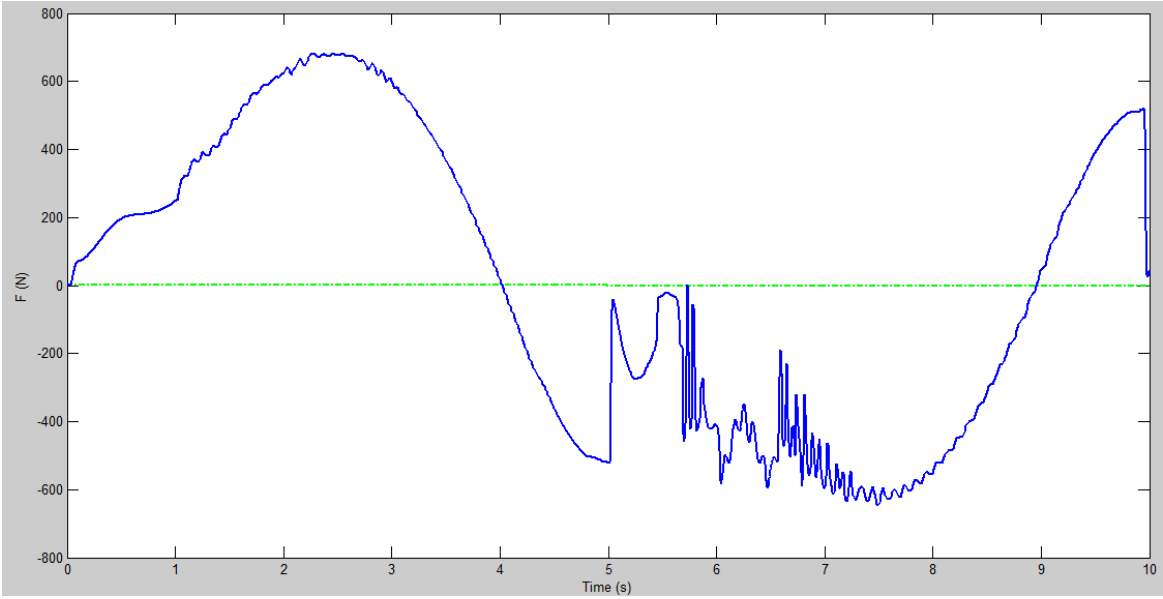

Fig 3.20: Input: Sine wave (0.1 m, 1Hz)

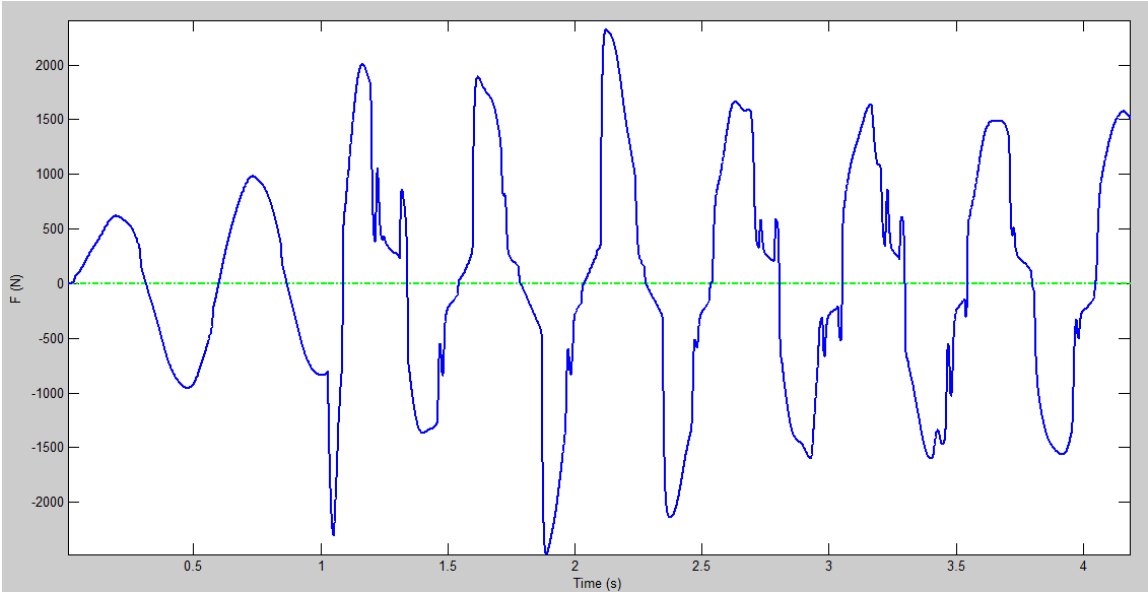

Fig 3.21: Input: Sine wave (0.1 m, 2Hz)

3.6.2. Pulse Road Input

The road input was taken as a pulse with amplitude of 0.1m and width of 0.57s.

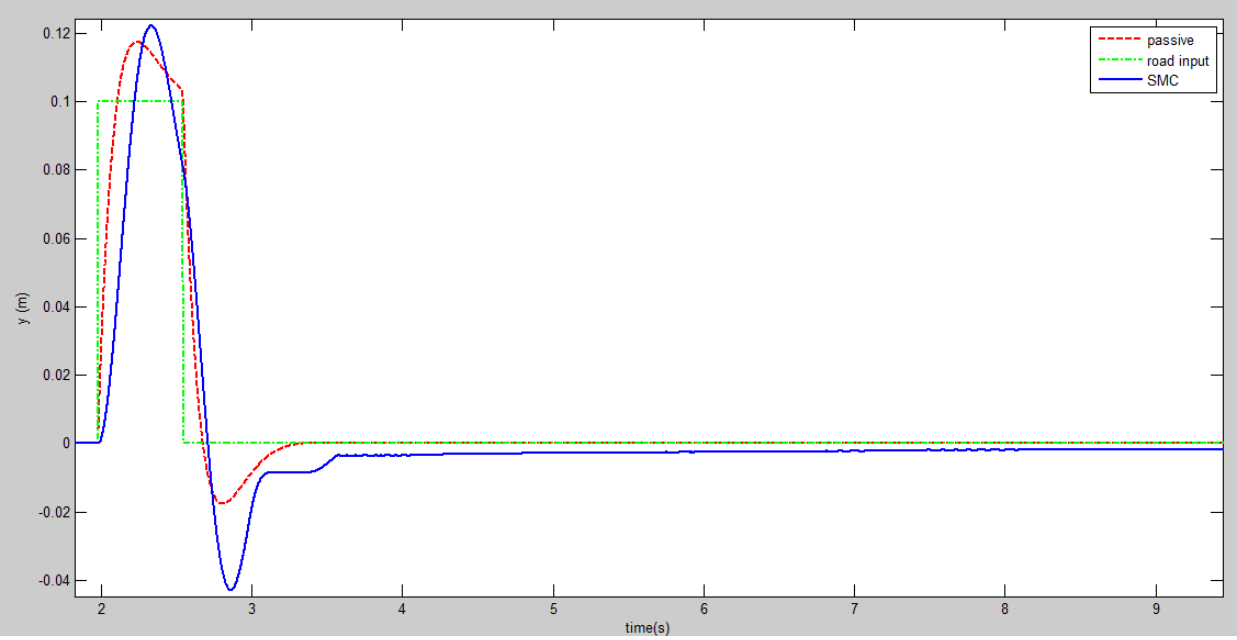

Fig 3.22: Displacement of sprung mass for Pulse Road input

In Figure 3.22, it is seen that the maximum overshoot of the output of the SMC system is more than the passive system in both the positive and negative directions, i.e., 0.1225 and -0.043m for SMC and 0.1175 and -0.018m for passive system. The settling time for SMC (6.38s) is almost twice as that of the passive system (3.36s).

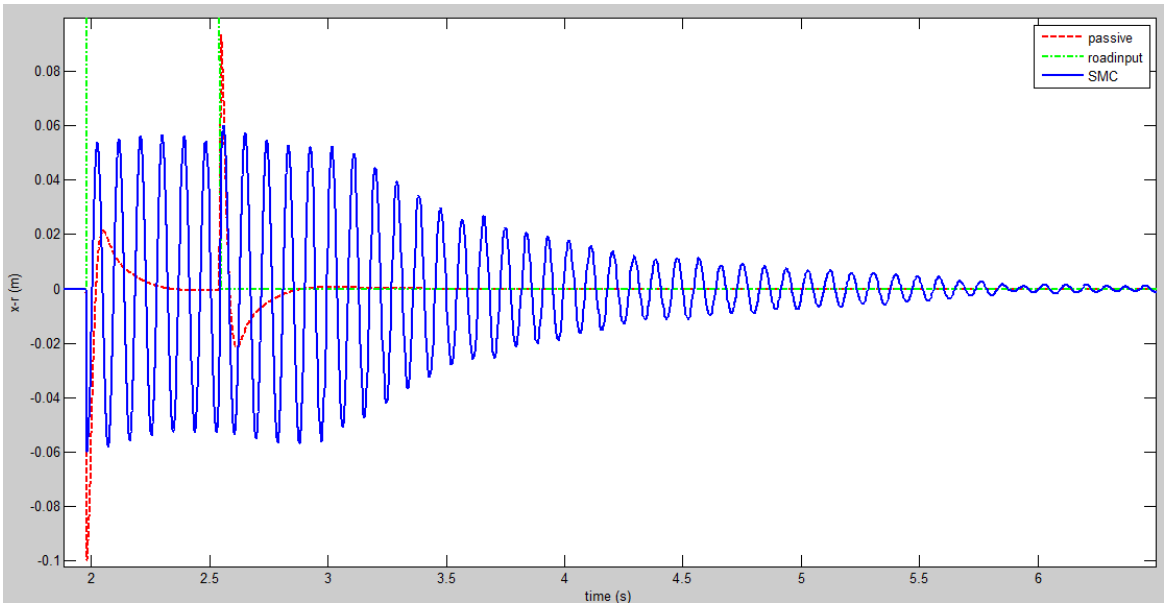

Fig 3.23: Difference in displacements of unsprung mass and road input for Pulse input

As illustrated in Fig 3.23, the value of (x-r) for SMC system reduces from 0.0599m to zero in 5.99s, where as, the same reduces from 0.0935m to zero in 3.27s. The same in case of SMC controlled damper sees a lot of oscillations.
Hence, the controller doesn't help in road handling. The road comfort parameters are in desirable limits but not better than passive system. These output present as a drawback to this system, the response time taken is not apt and the controller should make the damping better by taking other parameters into consideration.

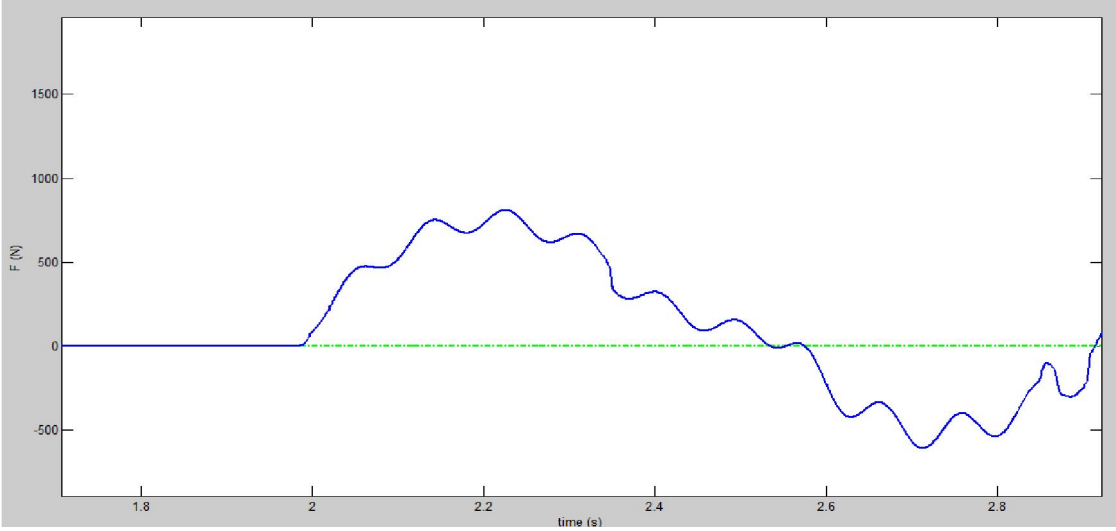

Fig 3.24: Force exerted by semi-active damper for Pulse input

3.6.3. Step Road Input

The road input was taken as a pulse with amplitude of 0.1m at time 5s.

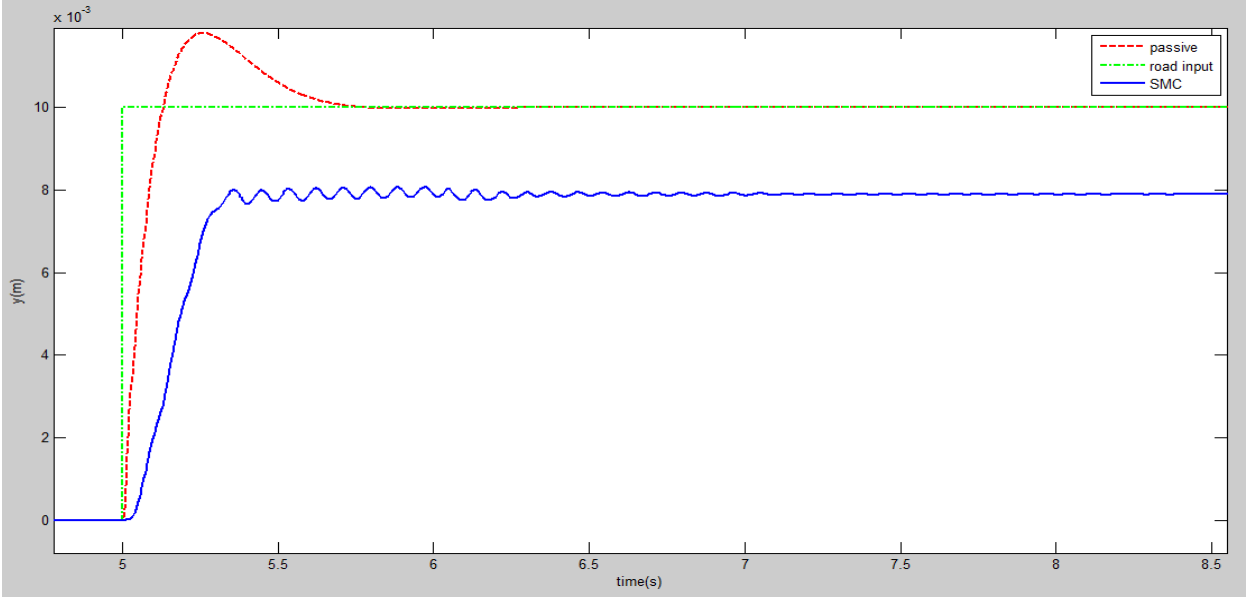

Fig 3.25: Displacement of sprung mass for Step Road input

In Figure 3.25, it is seen that the maximum overshoot of the output of the SMC system is less than the passive system, i.e., 0.08m for SMC and 0.118 for passive system.

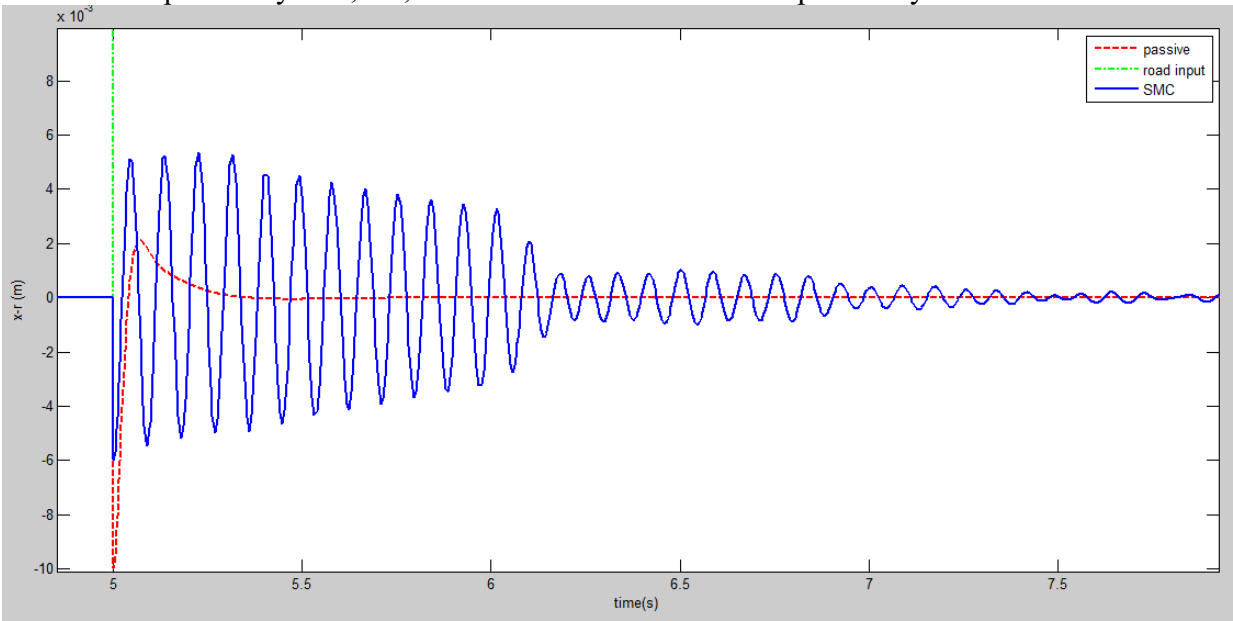

Fig 3.26: Difference in displacements of unsprung mass and road input for Step input

As illustrated in Fig 3.26, the value of (x-r) for SMC system reduces from 0.051m to zero in 7.52, where as, the same reduces has an overshoot of -0.099m in case of passive. However the settling time of passive is better (5.42s) and it doesn't have as many oscillations.

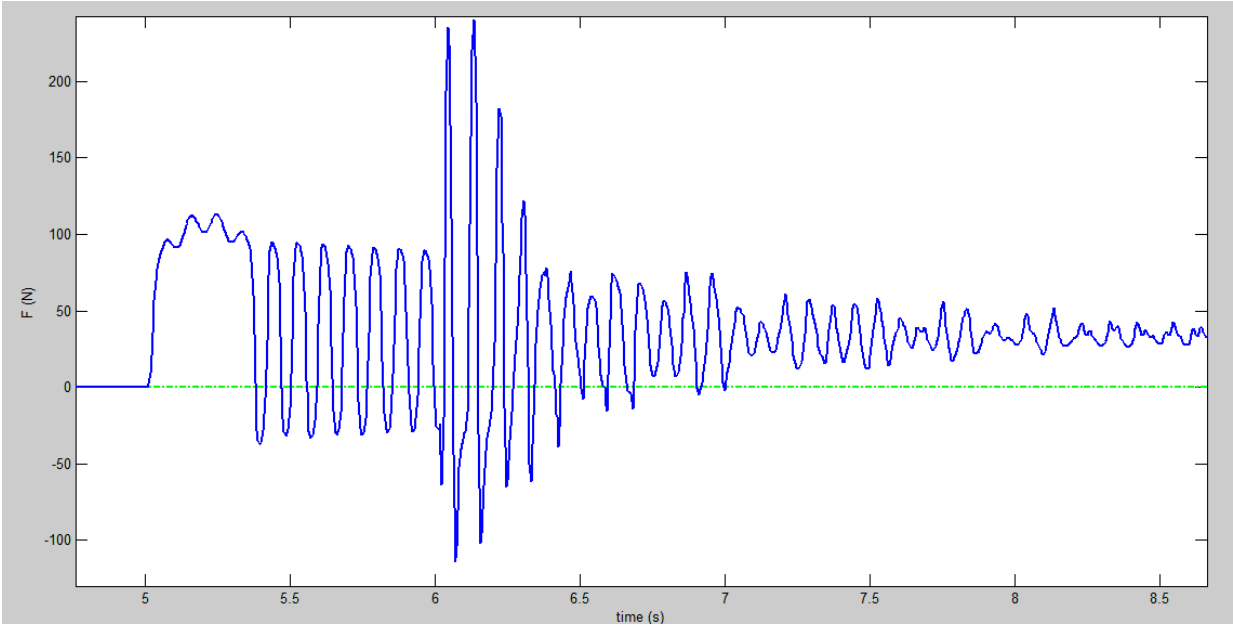

Fig 3.27: Force exerted by semi-active damper for Step input

APPENDIX

Parameters for Quarter Car Model

Parameter Name	Parameter Notation	Parameter Value
Sprung Mass	m_s	240 kg
Un-sprung Mass	m_u	36 kg
Stiffness of suspension	k_s	16000N/m
Stiffness of un-spring mass (tire)	k_t	160000 N/m
Constant G	G	0.0018

Parameters for Bouc-Wen Model

Parameter Name	Parameter Notation	Parameter Value
Parameters of the Hysteresis shape	γ, β, A, η	1, 0, 1.5, 2
Stiffness of the spring element	K_0	300 N/m
Input Voltage (u)	v	5 V
Other Parameters	$C_{0a}, C_{0b}, \alpha_{0a}, \alpha_{0b}$	4400, 442, 10872, 49616
Pre-yield stress	f_0	0 N
Other Parameters	k_2, I_0	10.092, 0.069

Parameters for Active Half car model

Parameter Name	Parameter Notation	Parameter Value
Sprung Mass	m_b	430 kg
Front wheel Mass	m_f	30 kg
Rear wheel mass	m_r	25kg
Stiffness of un-spring mass (tire)	$k_{1r}, k_{1f}, k_{2r}, k_{2f}$	152,152,6666.67,10000(kN/m)
Moment of inertia	I_b	600 kgm^2
Length of car body	a, b	1.469, 087m

REFERENCES

1) Half Car

(i) International Journal of Computer Applications (0975 - 8887) Volume 155, 2016:
Haifa Souilem, Sonia Mahjoub, Nabil Derbel, *Sliding Mode Control of Half-car Active Suspension*

(ii) Asian Journal of Control, Vol. 7, 2005:
Yahaya Md. Sam, Johari Halim Shah Bin Osman, *Modeling and control of the active suspension system using proportional integral sliding mode approach*

2) Quarter Car

(i) International Conference on Nascent Technologies in the Engineering Field, 2017:
S. M. Khot, Shradha Patil and Nikhil A. Bhaye, *Simulation study of MR Damper for Bump Road Profile*

(ii) Chinese Journal Of Mechanical Engineering, 2015:
Zhang Hailong, Wang Enrong, Zhang Ning, Min Fuhong, Subash Rakheja, Su Chunyi, *Semi-active Sliding Mode Control of Vehicle Suspension with Magneto-rheological Damper*

(iii) Mahmoud El-Kafafy, Samir M. El-Demerdash, Al-Adl Mohamed Rabeih, *Automotive Ride Comfort Control Using MR Fluid Damper*